AD-A146 431 INFLUENCE OF CONSOLIDATION SHEAR STRESSES AND RELATIVE DENSITY ON THRESHO..(U) RENSSELAER POLYTECHNIC INST TROY NY DEPT OF CIVIL ENGINEERING.. R DYVIK ET AL. 1/1

UNCLASSIFIED JUL 84 WES/MP/GL-84-15 DACW39-82-M-1600 F/G 8/13 NL

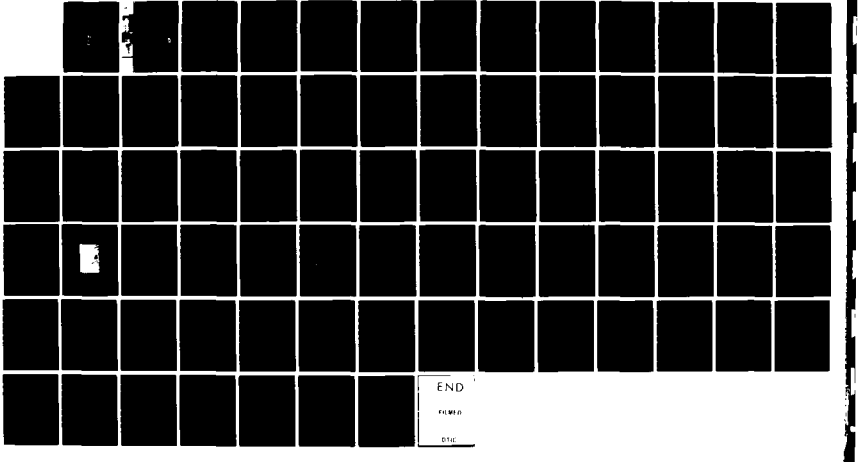

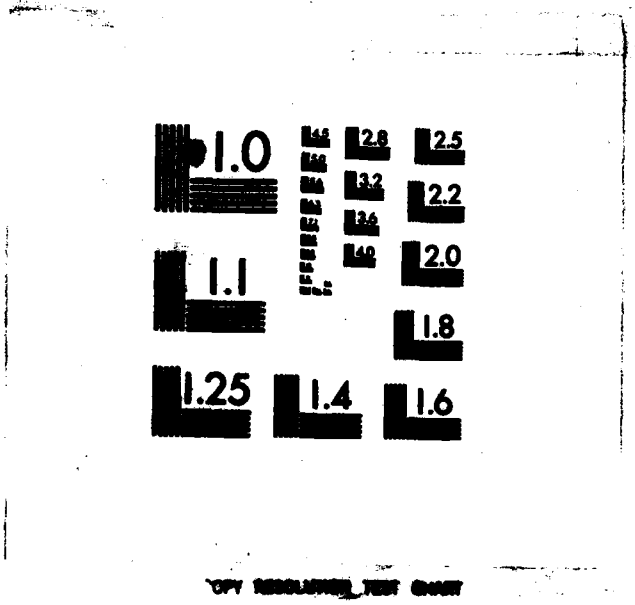
1.0
2.8
2.5
3.2
2.2
3.6
4.0
2.0
1.1
1.8
1.25
1.4
1.6

AD-A146 431

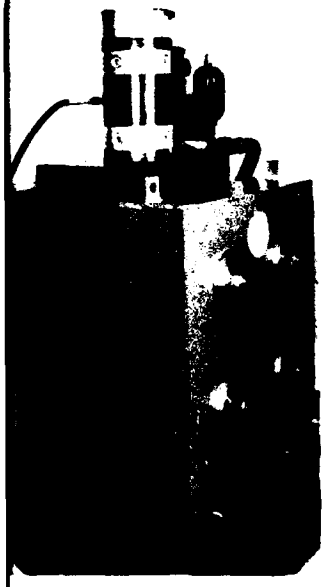

MISCELLANEOUS PAPER GL-84-15

INFLUENCE OF CONSOLIDATION SHEAR STRESSES AND RELATIVE DENSITY ON THRESHOLD STRAIN AND PORE PRESSURE DURING CYCLIC STRAINING OF SATURATED SAND

by

Rune Dyvik, Ricardo Dobry,
Gregory E. Thomas, William G. Pierce

Department of Civil Engineering
Rensselaer Polytechnic Institute
Troy, New York 12181

DTIC ELECTE OCT 0 9 1984 S D E

July 1984
Final Report

Approved For Public Release; Distribution Unlimited

DTIC FILE COPY

Prepared for DEPARTMENT OF THE ARMY
US Army Corps of Engineers
Washington, DC 20314

Under Purchase Order DACW 39-82-M-1600
(CWIS Work Unit 31666)

Monitored by Geotechnical Laboratory
US Army Engineer Waterways Experiment Station
PO Box 631, Vicksburg, Mississippi 39180-0631

84 10 04 079

Destroy this report when no longer needed. Do not return it to the originator.

The findings in this report are not to be construed as an official Department of the Army position unless so designated by other authorized documents.

The contents of this report are not to be used for advertising, publication, or promotional purposes. Citation of trade names does not constitute an official endorsement or approval of the use of such commercial products.

Unclassified
SECURITY CLASSIFICATION OF THIS PAGE (When Data Entered)

REPORT DOCUMENTATION PAGE	READ INSTRUCTIONS BEFORE COMPLETING FORM
1. REPORT NUMBER: Miscellaneous Paper GL-84-15	2. GOVT ACCESSION NO.: AD-A146 431
	3. RECIPIENT'S CATALOG NUMBER:
4. TITLE (and Subtitle): INFLUENCE OF CONSOLIDATION SHEAR STRESSES AND RELATIVE DENSITY ON THRESHOLD STRAIN AND PORE PRESSURE DURING CYCLIC STRAINING OF SATURATED SAND	5. TYPE OF REPORT & PERIOD COVERED: Final report
	6. PERFORMING ORG. REPORT NUMBER:
7. AUTHOR(s): Rune Dyvik, Ricardo Dobry, Gregory E. Thomas, William G. Pierce	8. CONTRACT OR GRANT NUMBER(s):
9. PERFORMING ORGANIZATION NAME AND ADDRESS: Rensselaer Polytechnic Institute, Department of Civil Engineering, Troy, New York 12181	10. PROGRAM ELEMENT, PROJECT, TASK AREA & WORK UNIT NUMBERS: Purchase Order DACW 39-82-M-1600 (CWIS Work Unit 31666)
11. CONTROLLING OFFICE NAME AND ADDRESS: DEPARTMENT OF THE ARMY, US Army Corps of Engineers, Washington, DC 20314	12. REPORT DATE: July 1984
	13. NUMBER OF PAGES: 71
14. MONITORING AGENCY NAME & ADDRESS(if different from Controlling Office): US Army Engineer Waterways Experiment Station, Geotechnical Laboratory, PO Box 631, Vicksburg, Mississippi 39180-0631	15. SECURITY CLASS. (of this report): Unclassified
	15a. DECLASSIFICATION/DOWNGRADING SCHEDULE:

16. DISTRIBUTION STATEMENT (of this Report)

Approved for public release; distribution unlimited.

17. DISTRIBUTION STATEMENT (of the abstract entered in Block 20, if different from Report)

18. SUPPLEMENTARY NOTES

Available from National Technical Information Service, 5285 Port Royal Road, Springfield, Virginia 22161.

19. KEY WORDS (Continue on reverse side if necessary and identify by block number)

Shear strength of soils (LC)
Soil liquefaction (LC)
Soil consolidation (LC)
Sandy soils (LC)
Pore Pressure (WES)
Alternating loads (WES)

20. ABSTRACT (Continue on reverse side if necessary and identify by block number)

In the last few years, a cyclic strain approach to pore pressure buildup and liquefaction during earthquakes of saturated cohesionless soils has been proposed and developed at Rensselaer Polytechnic Institute (RPI) and at other organisations. One of the key findings has been the existence, for every potentially liquefiable site and sand layer, of a "threshold ground surface acceleration," a_t, below which there is no pore pressure buildup. The value of a_t is mainly a function of two soil parameters: the "threshold shear strain"

(Continued)

DD FORM 1 JAN 73 1473 EDITION OF 1 NOV 65 IS OBSOLETE

Unclassified
SECURITY CLASSIFICATION OF THIS PAGE (When Data Entered)

a sub t

20. ABSTRACT (Continued).

of the sand, γ_t, and its maximum shear modulus, G_{max}. The existence of γ_t has been detected by several researchers in a number of laboratory studies. Also, the existence of γ_t and its range of values for quartz sands has been predicted from simple particulate mechanics considerations.

A previous experimental study of factors affecting the value of γ_t was conducted on Monterey No. 0 sand by R. S. Ladd at Woodward-Clyde Consultants. That study was performed on isotropically consolidated triaxial specimens having relative densities D_r, between 45 and 80 percent. The results revealed that (a) $\gamma_t = 1.1 \times 10^{-2}$ percent for normally consolidated (NC) specimens ranging in density from 45 to 80 percent, and consolidated isotropically under pressures ranging from 500 psf to 4,000 psf, and (b) for isotropically overconsolidated specimens and $D_r = 60$ percent, γ_t increases as the overconsolidation ratio, OCR, increases, with $\gamma_t = 2.9 \times 10^{-2}$ percent for OCR = 8.

The work presented herein was performed at RPI and constitutes an extension of the experimental study by Ladd and focuses on the effects of anisotropic consolidation and of very low relative densities on γ_t and on the rate of pore pressure buildup at cyclic strains slightly above γ_t. Two sands, Monterey No. 0 sand and Banding Sand, were tested and the results are reported herein. The effect of anisotropic consolidation is important because NC sands in the field are typically anisotropically consolidated, and also because any attempt to extend the cyclic strain approach to earth structures and slopes must necessarily consider the effect of consolidation shear stresses. Testing very loose sand, $D_r = 20$ percent, is important because very loose sand deposits in the field are usually the most susceptible to pore pressure buildup and liquefaction during earthquakes.

PREFACE

The work described in this report was performed under Purchase Order No. DACW 39-82-M-1600 as part of work being performed at the U. S. Army Engineer Waterways Experiment Station (WES), Vicksburg, Mississippi, on "Dynamic Properties of Well-Graded Soils," with funds provided by the Office, Chief of Engineers (OCE), U. S. Army, under CWIS Work Unit 31666. The OCE Technical Monitor was Mr. Richard F. Davidson.

This report was prepared by Dr. Rune Dyvik, Professor Ricardo Dobry, Mr. Gregory E. Thomas, and Professor William G. Pierce. The authors gratefully acknowledge the contributions of Ms. Mary E. Hynes-Griffin, WES, and Mr. Richard S. Ladd, Woodward-Clyde Consultants, in the planning and interpretation of the tests reported herein. The authors are also grateful to Mr. Mladen Vucetic for his help in conducting some of the tests.

The work reported herein was monitored by Ms. Mary E. Hynes-Griffin, Earthquake Engineering and Geophysics Division (EEGD), Geotechnical Laboratory (GL), WES, under the general supervision of Dr. Arley G. Franklin, Chief, EEGD, and Dr. William F. Marcuson III, Chief, GL.

COL Tilford C. Creel, CE, was Commander and Director of WES during the period of study. Mr. F. R. Brown was Technical Director.

Accession For	
NTIS GRA&I	☒
DTIC TAB	☐
Unannounced	☐
Justification	
By	
Distribution/	
Availability Codes	
Dist	Avail and/or Special
A-1	

DTIC COPY INSPECTED 1

CONTENTS

CONVERSION FACTORS, U. S. CUSTOMARY TO METRIC (SI) UNITS OF MEASUREMENT

U. S. customary units of measurement used in this report may be converted to metric (SI) units as follows:

Multiply	By	To Obtain
gallons (U. S. liquid)	3.785412	cubic decimeter
inches	2.54	centimetres
inch-pounds (force)	0.1129848	metre-newtons
kips (force) per square foot	47.88026	kilopascals
pounds (force)	4.448222	newtons
pounds (force) per square foot	47.88026	pascals
pounds (force) per square inch	6894.757	pascals
pounds (mass) per cubic foot	16.01846	kilograms per cubic metre

INFLUENCE OF CONSOLIDATION SHEAR STRESSES AND RELATIVE DENSITY ON THRESHOLD STRAIN AND PORE PRESSURE DURING CYCLIC STRAINING OF SATURATED SAND

CHAPTER 1

INTRODUCTION

In the last few years, a cyclic strain approach to pore pressure buildup and liquefaction of saturated cohesionless soils during earthquakes has been proposed and developed at Rensselaer Polytechnic Institute (RPI) and at other organizations (Dobry and Ladd, 1980; Dobry et al., 1980, 1981, 1981a, 1982). One of the key findings has been the existence, for every potentially liquefiable site and sand layer, of a "threshold ground surface acceleration," a_t, below which there is no pore pressure buildup. The value of a_t is mainly a function of two soil parameters: the "threshold shear strain" of the sand, γ_t, and its maximum shear modulus, G_{max}. The existence of a_t has been confirmed by field measurements in Japan (Ishihara, 1981), while γ_t has been detected by several researchers in a number of laboratory studies. Also, the existence of γ_t and its range of values for quartz sands has been predicted from simple particulate mechanics considerations (Dobry et al., 1982).

A previous experimental study of factors affecting the value of γ_t was conducted on Monterey No. 0 sand by R.S. Ladd at Woodward-Clyde Consultants, Clifton, N.J. That study was performed on isotropically consolidated triaxial specimens having relative densities, D_r, between 45% and 80%. The results, reported by Dobry

et al. (1981,1982), revealed that: a) $\gamma_t = 1.1 \times 10^{-2}\%$ for normally consolidated (NC) specimens ranging in density from 45% to 80%, and consolidated isotropically under pressures ranging from 500 psf* to 4,000 psf, and b) for isotropically overconsolidated specimens and $D_r = 60\%$, γ_t increases as the overconsolidation ratio, OCR, increases, with $\gamma_t = 2.9 \times 10^{-2}\%$ for OCR = 8.

The work presented herein was performed at RPI and constitutes an extension of the experimental study mentioned in the previous paragraph. It focuses on the effects of anisotropic consolidation and of very low relative densities on γ_t and on the rate of pore pressure buildup at cyclic strains slightly above γ_t. Two sands, Monterey No. 0 sand and Banding Sand were tested and the results are reported herein. The effect of anisotropic consolidation is important because NC sands in the field are typically anisotropically consolidated, and also because any attempt to extend the cyclic strain approach to earth structures and slopes must necessarily consider the effect of consolidation shear stresses. Testing very loose sand, $D_r = 20\%$, is important because very loose sand deposits in the field are usually the most susceptible to pore pressure buildup and liquefaction during earthquakes.

---

* A table of factors for converting U. S. customary units of measurement to metric (SI) units is presented on page 3.

CHAPTER 2

TESTING EQUIPMENT

2.1 Equipment Description

The cyclic soil testing system located in the Class of 1933 Earthquake Engineering and Cyclic Loading Laboratory at RPI was used to perform the tests in this study. This system is based on a servo-hydraulic closed-loop testing system which was manufactured for RPI by MTS Systems Corporation and is shown in Fig. 1.

The cyclic triaxial system consists of an axial and a torsional actuator located at the top of the same frame. The two actuators are connected in series by a yoke system but are operated by separate controllers. This provides the capability of performing cyclic axial triaxial (usually called cyclic triaxial in the geotechnical literature), cyclic torsional triaxial or combined cyclic axial-torsional triaxial tests on the soil specimen. Either of the modes can be operated monotonically or cyclically in either stress- or strain-controlled conditions. Additionally, if a combined cyclic axial-torsional triaxial test is run, an arbitrary phase angle may be specified between the two modes, which can be anywhere from 0 to 360 degrees.

The loads are measured and recorded through a single axial/torsional load cell. Each actuator is provided with an internal displacement transducer, but due to the great resolution and minimum system compliance error required for the threshold measurements, a

very accurate LVDT was mounted on the triaxial cell close to the soil specimen and is used for the threshold tests. Excess pore water pressures within the specimen are measured by means of a very stiff pressure transducer, which is connected to the specimen through high quality stainless steel ball valves and short lengths of 1/8 inch copper tubing.

The piston entering the triaxial cell rides on an air bearing to reduce errors in the load readings due to friction. Brass porous stones with coarse surfaces are screwed into the triaxial cell platens so as to completely transfer the torque and torsional angle applied to the cell piston.

Data are recorded on an 18 channel light pen oscillograph and an X-Y-Y plotter. The data are first digitized manually, and then reduced, manipulated and plotted by computer.

2.2 Equipment Capabilities

Although the frequency capabilities are a function of system gain and actuator displacement amplitude, the range of most interest in geotechnical studies is easily covered by the equipment used (from several minutes per cycle to 5-10 Hz). Very large accumulators are incorporated into the system (5 gallons feed, 2.5 gallons return oil), to provide good control and performance at large strains and high frequencies. All cyclic tests in this study were performed at a

frequency of 1 Hz.

The MTS electronics are set up in such a way that there are four ranges (1, 2, 3 and 4) where full scale output is 100%, 50%, 20% and 10%, respectively, of the full scale capabilities of the measuring system. The following is a list of the capabilities of range 1, and of the resolution of range 4, for the components used in this study:

Mode	Parameter	Max. Capability (Range 1)	Resolution (Range 4)
Axial	Load	± 1,000 lb	1×10^{-2} lb
Axial	Displacement	± 0.1 in	1×10^{-6} in
Torsional	Torque	± 500 in.lb.	5×10^{-3} in.lb.
Torsional	Angle	± 50 degrees	5×10^{-4} degrees
-	Excess Pore Pressure	+ 200 psi	2×10^{-3} psi

Every test in this study was performed in range 4 (the finest) so as to attain the maximum resolution. See Appendix A for details about the measurement system and its calibration.

CHAPTER 3

TESTING PROCEDURE AND CALCULATIONS

Previous results from similar tests performed at RPI have been compared to existing high-quality results from other researchers (Thomas, et al., 1982), with excellent agreement. It is therefore felt that the equipment, specimen preparation and testing procedures and techniques used herein are of similar high quality.

The reconstituted triaxial sand specimens tested were all solid cylinders 2.0 inches in diameter and 4.0 inches in height. They were prepared by the wet tamping technique (Ladd, 1978), using six undercompacted lifts at 6 percent water content. This method was chosen to increase the degree of uniformity of the relative density, both within each specimen and between different specimens.

The triaxial cell was filled with deaired water to prevent migration of air through the specimen membrane. The specimen was then flushed with CO_2 and filled with deaired distilled water. The specimen was backpressured overnight at 62 psi with an effective all-around confining pressure of 3 psi.

The next day, the specimen was consolidated to the desired k_c ($= \bar{\sigma}_{vo}/\bar{\sigma}_{ho}$), with $\bar{\sigma}_{ho}$ always being 2 ksf. Volume and height changes were recorded during consolidation.

After consolidation, the triaxial cell was sealed, the piston was locked in place, and the cell was transferred to the testing frame. Here it was fixed to the table, and attached to the actuator, the volume change burette and the pore pressure transducer.

The pore pressure response (B factor) was then determined to check for adequate system saturation. This was done by increasing the cell pressure by 2 psi and measuring the pore pressure increase in the specimen. If the measured value of B was less than 95%, the lines were resaturated and the procedure was repeated until adequate saturation was obtained.

Consolidation to a desired value of k_c, as described above, provided stress conditions where the maximum cyclic shear stresses would occur on the same plane as the maximum static (consolidation) shear stresses within the specimen. Cases with the maximum cyclic and static shear stresses on different planes within the specimen were also studied by first isotropically consolidating (k_c = 1.0) the specimen; then, after hookup to the frame was completed, an additional static torque was slowly applied to the specimen and consolidation was allowed to finish under this torque.

The drainage valves were then closed, the connection between the pore pressure transducer and the specimen was opened, and the cyclic test was started.

The method used for determining the threshold shear strain (γ_t) of each specimen was to run a succession of short cyclic sequences of 5 sinusoidal axial strain cycles at a frequency of 1 Hz. Each sequence was run at a higher cyclic axial strain, until a residual pore pressure greater than zero was measured. The cyclic axial strain needed to induce this small residual pore pressure is the

axial threshold strain, ε_{at}. During the undrained cyclic triaxial tests, the cyclic axial strain, ε_a, was measured, and the cyclic shear strain, γ_c, was calculated from:

$$\gamma_c = 1.5\ \varepsilon_a$$

which assumes constant volume testing and isotropic or cross-anisotropic soil. Correspondingly, the threshold shear strain is calculated from $\gamma_t = 1.5\ \varepsilon_{at}$. Once the threshold strain was determined, additional short cyclic sequences of 5 axial cycles each were performed at cyclic strains slightly above the threshold, and the residual pore pressure was measured at the end of the five cycles. Reconsolidation of the specimen was allowed in all cases after each of these sequences, both below and above the threshold. Below the threshold there was never any noticeable volume or height change. Above the threshold slight volume changes and specimen height changes were measured. Cyclic testing was stopped when the accumulated specimen volumetric strain due to cycling reached 0.5%.

Very little or no degradation of the secant Young's modulus, E, was observed in all the tests within a given 5-cycle sequence, both below and above the threshold. Therefore, for the strains and numbers of cycles used in this study, these sequences can be considered either as stress- or strain-controlled tests. Due to the

mechanical and electronic characteristics of the equipment, better control and resolution is attained in stress-control. Therefore all tests were run in the stress-controlled mode, but they can be considered to be strain-controlled tests also. For specimens with $k_c > 1.0$ tested at strains larger than the threshold, some minor offsetting of the cyclic strain (decrease in specimen height) was observed, but the measured peak to peak strain amplitude was very constant in all cases. These very small offsets for the $k_c > 1.0$ tests were ignored in the cyclic shear strain calculations.

CHAPTER 4

APPLIED STRESSES

A main purpose of this study is to investigate the influence of consolidation shear stresses on the behavior of saturated sand subjected to small strain undrained cyclic loading. The stress conditions applied to the specimens in this study, both at the end of consolidation and during cyclic loading, are discussed in this section. As pointed out previously, these small strain cyclic sequences can be considered to be both strain- and stress-controlled tests. In this chapter, the stress aspect is emphasized while in the rest of the report the results are discussed in terms of the induced strains.

Tests performed on isotropically consolidated specimens are taken as a reference. Figure 2a shows the isotropic stress conditions after the specimen has been consolidated, with $\bar{\sigma}_{vo}$ = effective vertical stress after consolidation and $\bar{\sigma}_{ho}$ = effective horizontal stress after consolidation. For the isotropically consolidated case ($k_c = \bar{\sigma}_{vo}/\bar{\sigma}_{ho} = 1.0$), the Mohr circle is a point. Figure 2b shows the state of total stress as the specimen is being subjected to symmetric cyclic axial loading around a zero initial deviator stress. The Mohr circles correspond to maximum compression $(\sigma_v)_{max}$ and maximum extension $(\sigma_v)_{min}$ axial loads and the 45° line is the total stress path for the specimen as the loading alternates between $(\sigma_v)_{max}$ and $(\sigma_v)_{min}$.

Figure 3a shows the stress conditions for a specimen anisotropically consolidated to a $k_c = \bar{\sigma}_{vo}/\bar{\sigma}_{ho} > 1.0$. Figure 3b shows the case where the anisotropically consolidated specimen is

subjected to cyclic deviator stresses less than the initial static deviator stress and the specimen remains in compression throughout (incomplete stress reversal) and the principal planes remain unchanged. Figure 3c presents the case when the cyclic deviator stress is greater than the static stress and the specimen experiences extension unloading (complete stress reversal). In this case the major principal stress direction rotates 90° during each cycle. In the tests reported herein, both situations sketched in Figs. 3b and 3c did occur. During the axial cyclic testing without a static torque, depicted in Figures 2 and 3, the principal directions of stress remain vertical and horizontal during consolidation and cyclic loading. Therefore, both the maximum consolidation shear stress and the maximum cyclic shear stress occur on the same planes, which are ± 45° planes.

Both types of test shown in Figs. 2 and 3 were consolidated with zero torque, T = 0. Figure 4a shows the Mohr circle for a specimen that has been "isotropically" consolidated in the vertical and horizontal directions, "k_c" = 1, but which has a consolidation shear stress provided by an applied torque, T ≠ 0. (Of course, if T ≠ 0 the specimen has not been really isotropically consolidated, even if $\bar{\sigma}_{ho} = \bar{\sigma}_{vo}$). This circle corresponds to the outer edge of the specimen, where τ_{max} is the shear stress induced by T at this location. This maximum shear stress can be determined if it is assumed, in first approximation, that the soil material is isotropic and

linearly elastic:

$$\tau_{max} = Tr/J = Tr/(0.5\pi r^4) = 2T/(\pi r^3)$$

where J is the polar moment of inertia, r is the radius of the solid specimen, and T is the applied torque. Due to the fact that the soil is nonlinear, the previous expression will in general slightly overestimate the value of τ_{max}, with the error becoming larger for values of T near failure of the soil.

Figure 4b shows the stress conditions as a vertical (deviator) cyclic stress is applied to a specimen with an applied torque. In this case, cyclic loading induces a rotation different from 90° from the major principal direction of stress, and the maximum cyclic shear stresses occur in planes which are different from the vertical/horizontal planes which contained the maximum consolidation shear stresses.

CHAPTER 5

SANDS TESTED

Two sands were used in this study: Monterey No. 0 sand and Banding sand. The Banding sand is the finer of the two as shown by the grain size distribution curves for each sand in Figure 5. Both soils are uniform, clean quartz sands. The Monterey No. 0 sand is a commercially available washed uniform medium-to-fine beach sand, composed of quartz and feldspar particles, and which has been extensively used for geotechnical earthquake engineering studies (e.g. Pyke et al., 1974; Mulilis et al., 1975; Dobry et al., 1982; Thomas et al., 1982). The Banding sand is also a commercially available sand presently sold by the Ottawa Silica Co., Ottawa, Illinois under the trade name "F-75". Banding sand has also been used previously in liquefaction studies (Castro, 1969; Geotechnical Engineers, 1982). Selected index properties of each sand are presented in Table 1. Except for the difference in the values of D_{50}, the two sands are very similar.

CHAPTER 6

TESTING PROGRAM

A total of 22 tests were performed on specimens of Monterey No. 0 sand and Banding sands. Of these, thirteen tests were on Monterey No. 0 and nine tests were on Banding sand. Tests were performed on medium-dense (D_{rf} ≈ 60%) and loose (D_{rf} ≈ 20%) sand specimens. These values of relative density, D_{rf}, are after consolidation. The test program focused mainly on the Monterey No. 0 sand, for which a larger number of tests were conducted and a greater variation of the consolidation stress parameters was allowed. A more limited testing program on Banding sand was also performed, mainly to determine the influence of grain size on the results.

Tables 2a and 2b summarize the specimen and test characteristics in each of these twenty-two tests on Monterey No. 0 sand and Banding sand, respectively.

The first column in each of these two tables lists the value of D_{rf} for each specimen after consolidation. Each specimen was prepared with an initial relative density as close to 20% or 60% as possible, but small variations in the specimen preparation as well as the consolidation process itself yielded measured values of D_{rf} between about 22% and 30%, and between 56% and 68%, respectively. These variations in values of D_{rf} did not seem to affect the results noticeably.

The second column in Tables 2a and 2b is the B-parameter (pore pressure response) measured in each specimen. All values are

between 97 and 99.6%, indicating a high degree of saturation.

Columns three and four indicate the consolidation horizontal and vertical stresses. The horizontal effective confining stress, $\bar{\sigma}_{ho'}$ was 2 ksf in all tests, while k_c values between 1.0 and 2.5 were used. For the Monterey No. 0 sand, k_c values of 1.0, 1.5, 2.0 and 2.5 were utilized; notice that this last value of k_c = 2.5 corresponds to a K_o = 0.4, which is approximately the expected in-situ K_o for level, normally consolidated sand deposits. For the Banding sand, tests were performed with k_c = 1.0 and 2.0.

Column five indicates the magnitude of the torque applied to the specimen during consolidation. In most of the tests, T = 0, but in two of the tests on Monterey No. 0 sand a torque T = 7.28 in-lb was used. This value of T was chosen in order to achieve a mobilized friction angle at the outermost edge of the specimen about equal to the mobilized friction angle for the tests with T = 0 and k_c = 2.0, with both friction angles calculated at the end of consolidation.

As can be observed in Tables 2a and 2b, several tests were duplicated to check the repeatability of the results. One of the tests on Monterey No. 0 sand at D_{rf} ≈ 60% (k_c = 2.0, T = 0) was also repeated, but with only one 5-cycle sequence at a relatively large shear strain above the threshold. This was done to verify the assumption that the preshaking effect associated with the staging of several 5-cycle sequences did not affect significantly the measured modulus and pore pressure.

CHAPTER 7

TEST RESULTS ON MONTEREY NO. 0 SAND

7.1 Tests with $k_c = 1.0$ and $T = 0$

A total of four tests were performed on Monterey No. 0 sand with $k_c = 1.0$ and $T = 0$. Of these, two tests were conducted on specimens with $D_{rf} = 20\%$ and two tests with $D_{rf} = 60\%$. The residual pore pressures measured in these tests are presented in Figures 6 through 9, while the Young's moduli are shown in Figures 10 and 11.

Figure 6 shows the normalized residual pore pressures, $u_r/\bar{\sigma}_{ho}$ measured for the two tests with $D_{rf} = 60\%$. Note the extremely fine scale of the residual pore pressure (ordinate) axis; no data point is higher than $u_r/\bar{\sigma}_{ho} = 0.02$. A threshold strain, $\gamma_t = 0.01\%$ is clearly defined. All data points in Figure 6 correspond to residual pore pressures measured after 5 uniform strain cycles ($n = 5$).

The data points in Figure 7 show similar results for the same sand, but for the two tests with $D_{rf} = 20\%$. The curve from Figure 6 for $D_{rf} = 60\%$ has been superimposed on Figure 7 for comparison. Figure 7 clearly shows that the threshold is $\gamma_t = 0.01\%$ for both $D_{rf} = 20\%$ and $D_{rf} = 60\%$, but that the residual pore pressures after 5 cycles, for $\gamma_c > \gamma_t$, are somewhat higher for $D_{rf} = 20\%$.

This value of $\gamma_t = 0.01\%$ for isotropically consolidated Monterey No. 0 sand is consistent with similar results obtained

previously for the same sand at the Woodward-Clyde Consultants laboratory for D_{rf} between 45% and 80% (Dobry et al., 1982), and later at RPI for D_{rf} = 60% (Thomas et al., 1982). Figure 7 extends this conclusion to sands looser than 45%, and shows that, for this sand, $\gamma_t \approx 0.01\%$ for $20\% \leq D_{rf} \leq 80\%$.

Figure 8 shows the normalized residual pore pressures for the same two tests with $D_{rf} \approx 60\%$ as in Figure 6, but with a compressed pore pressure scale ($u_r/\bar{\sigma}_{ho}$ up to 0.3). This figure shows residual pore pressures for higher shear strains not included in Figure 6. Again, all values of $u_r/\bar{\sigma}_{ho}$ in Figure 8 are after five uniform shear strain cycles, with reconsolidation between every 5-cycle sequence, and with γ_c always increasing from one sequence to the next. In Figure 8, it is interesting to note that, as γ_c increases, $u_r/\bar{\sigma}_{ho}$ first adopts non-zero values at $\gamma_c = \gamma_t \approx 0.01\%$, but remains very small until $\gamma_c \approx 0.015\%$, and then starts increasing faster for $\gamma_c > 0.015\%$. Therefore, Figure 8 suggests that, for some practical applications, an "engineering" value of γ_t ($\approx 0.015\%$ in this case), different and higher than $\gamma_t \approx 0.01\%$, may be used as a threshold marking the beginning of significant pore water pressure increases.

Figure 9 is similar to Figure 8 but for $D_{rf} \approx 20\%$. The curve drawn in this figure represents the data for $D_{rf} \approx 60\%$ from Figure 8. This comparison shows that $u_r/\bar{\sigma}_{ho}$ is larger at equal strains for $D_{rf} \approx 20\%$ than for $D_{rf} \approx 60\%$, once the threshold strain is exceeded.

Figure 10 shows the cyclic Young's Modulus, (1/2 peak to peak), E, normalized to the effective consolidation octahedral stress for the specimen, $\bar{\sigma}_{oct}$ [$=1/3(\bar{\sigma}_{vo} + 2\,\bar{\sigma}_{ho}) = (k_c+2)\bar{\sigma}_{ho}/3$], at $D_{rf} \approx$ 60%, and for the same two tests shown in Figures 6 and 8.

The data points in Figure 11 shows $E/\bar{\sigma}_{oct}$ for the same two tests at $D_{rf} \approx$ 20%, already presented in Figures 7 and 9. The curve for $D_{rf} \approx$ 60% from Figure 10 has been superimposed on Figure 11 for comparison. As expected, the modulus is lower for the looser specimens at all shear strains, but the trend of variation of declining $E/\bar{\sigma}_{oct}$ versus γ_c is similar for both relative densities.

7.2 Tests with $k_c > 1.0$ and $T = 0$

A total of seven tests were performed on anisotropically consolidated Monterey No. 0 sand specimens, with $1.5 \leq k_c \leq 2.5$ and $T = 0$. Four of these tests were conducted at relative densities, $D_{rf} \approx$ 60%, while three tests correspond to $D_{rf} \approx$ 20%.

Figures 12 and 13 present the residual pore pressures measured after 5-cycle loading sequences for $D_{rf} \approx$ 60% and $D_{rf} \approx$ 20%, respectively. In both figures, the data for $k_c = 1.5$ and 2.0 exhibit a similar threshold strain, $\gamma_t = 0.01\%$ to that of the isotropic case, which are also shown here for comparison. The behavior for $k_c = 2.5$ is more complex, with development of slightly negative pore pressures at shear strains immediately below 0.01%, and with development of positive pore pressures for strains larger than 0.01%

to 0.02%. The general trend in Figs. 12 and 13 is quite similar, with the pore pressure at a given strain decreasing as the value of k_c increases.

Figures 14 and 15 correspond to the same tests shown in Figures 12 and 13, respectively, but with a compressed pore pressure scale, and including data points for larger cyclic strains.

In most of the tests shown in Figs. 14 and 15, as well as in the rest of the tests listed in Tables 2a) and 2b), several 5-cycle loading sequences were applied to the specimen at increasing shear strains. For strains above the threshold, this staged cycling and pore pressure buildup, plus the reconsolidation between sequences, may have produced a "pre-shaking" effect on the specimen, which would tend to decrease the values of $u_r/\bar{\sigma}_{ho}$ measured in the final sequences, as compared with "virgin" specimens not subjected to preshaking. [For the preshaking effect, see e.g. Seed, et al., 1977] For the strains and numbers of cycles used in this investigation, it was assumed that this preshaking effect was small and did not have much effect on the measured values of $u_r/\bar{\sigma}_{ho}$. To verify this assumption, one of the tests on Monterey No. 0 sand, D_{rf} = 60% and k_c = 2.0 was repeated. In this test, first nondestructive measurements were performed at values of γ_c < 0.01%, and then a single 5-cycle sequence was conducted at γ_c = 0.11%. The corresponding residual pore pressure, plotted in Figure 14 as a single data point (large triangle), is thus unaffected by preshaking. The

comparison between this data point and the corresponding points for k_c = 2.0 shows that the preshaking effect on $u_r/\bar{\sigma}_{ho}$ was small and can be neglected.

The data points in Figures 16 and 17 show the normalized cyclic Young's Modulus, $E/\bar{\sigma}_{oct}$, for $k_c > 1.0$ and D_{rf} = 60% and D_{rf} = 20%, respectively. Curves for k_c = 1.0 for this sand, obtained from the results in Figs. 10 and 11, have been superimposed on Figures 16 and 17. The values of $E/\bar{\sigma}_{oct}$ at the larger strains in Figures 16 and 17 are very similar and independent of k_c for the range $1.0 \leq k_c \leq 2.5$. This is reasonable and consistent with the fact that both the modulus at large strains and the shear strength in sands have been found to vary linearly with effective confining pressure. However, at small strains, it should be expected that the data points for larger values of k_c would have somewhat lower values of $E/\bar{\sigma}_{oct}$ in Figs. 16 and 17. An inspection of these figures shows that this is exactly what happens.

7.3 Tests with k_c = 1.0 and T≠ 0

As explained previously, two tests were performed on Monterey No. 0 sand, in which $\bar{\sigma}_{ho} = \bar{\sigma}_{vo}$ = 2 ksf and a static torque, T = 7.28 in-lb was applied during consolidation. The two tests correspond respectively to D_{rf} = 60% and D_{rf} = 20%. In this way, a new situation was created, in which, unlike the previous tests with $k_c > 1.0$, the maximum static shear stress within the specimen

acts on different planes than those corresponding to the maximum cyclic shear stress. The value of T = 7.28 inch-pounds was chosen to cause a mobilized angle of friction at the end of consolidation, at the outer edge of the specimen, similar to that mobilized in the whole specimen during the tests with k_c = 2.0 and T = 0.

The data points in Figures 18 and 19 show the residual pore pressures measured in these "k_c" = 1.0, T ≠ 0 tests after 5-cycle sequences of uniform cyclic shear strain, for D_{rf} = 60% and D_{rf} = 20%, respectively. The curves superimposed on each figure correspond to k_c = 1.0 and T = 0 (from Figures 6 and 7).

The data points in Figures 20 and 21 present the pore pressures for the same two tests, but for a compressed normalized pore pressure scale and including additional data points at larger strains. Again, the curves in these two figures correspond to k_c = 1.0 and T = 0, and were obtained from Figures 8 and 9.

Figures 18 through 21 show that the threshold residual pore pressure is essentially the same for k_c = 1.0, with or without a moderate static torque applied during consolidation. The mobilized friction angle during consolidation in the tests with T = 7.28 in-lb varies between 0 at the center of the specimen to a value similar to that induced in the tests with k_c = 2 and T = 0, at the outer edge. Therefore, it should be expected that the data points in Figures 18 through 21 should agree closely with those for tests in which $1.0 \leq k_c \leq 2.0$ and T = 0. A comparison between data points in Figures 18

through 21 with those presented in Figures 12 through 15 indicate that the measurements of residual pore pressure versus strain, for a given relative density, are essentially identical between tests with T = 0 and k_c = 1.5 and tests with T = 7.28 in-lb. and "k_c" = 1.0.

The data points in Figures 22 and 23 show the values of $E/\bar{\sigma}_{oct}$ for the same two tests. The curves superimposed on the figures are for the basic isotropic case, k_c = 1.0 and T = 0 (from Figures 10 and 11). These figures show that the presence of the static torque decreases the modulus of the specimen.

CHAPTER 8

TEST RESULTS ON BANDING SAND

8.1 Tests with $k_c = 1.0$ and $T = 0$

A total of six tests were performed on the finer Banding sand with $k_c = 1.0$ and $T = 0$. Of these, three tests were conducted on specimens with $D_{rf} \approx 60\%$ and three tests with $D_{rf} \approx 20\%$. The residual pore pressures are presented in Figure 24. The comparison in Figure 24 shows that, in Banding sand, $\gamma_t = 0.8$ to $0.9 \times 10^{-2}\%$, independent of relative density for the range $20\% \leq D_r \leq 60\%$. Also, the residual pore pressures at $\gamma_c > \gamma_t$ are somewhat larger for the looser sand, $D_{rf} \approx 20\%$. This influence of D_{rf}, as shown, in Figure 24 for Banding Sand, is similar to that obtained for Monterey sand in Figure 7.

8.2 Tests with $k_c > 1.0$ and $T = 0$

The data points in Figures 25 and 26 show the results of the three tests performed on anisotropically consolidated Banding Sand specimens, with $k_c = 2.0$ and $T = 0$. Figure 25 includes two tests with $D_{rf} \approx 60\%$, while Figure 26 includes two tests with $D_{rf} \approx 20\%$.

Also plotted on Figures 25 and 26 are the results of the isotropically consolidated case, $k_c = 1.0$, $T = 0$, obtained from Figure

24. The comparisons in Figures 25 and 26 show that γ_t either does not change or increases slightly where k_c is increased from 1.0 to 2.0, and that the residual pore pressure for a strain, $\gamma_c > \gamma_t$ is lower for the anisotropically consolidated case, $k_c = 2.0$. These are entirely consistent with the conclusions for Monterey No. 0 sand, discussed previously in conjunction with Figures 12 and 13.

CHAPTER 9

SUMMARY AND CONCLUSIONS

A total of twenty-two undrained cyclic triaxial (axial) tests were performed on saturated specimens of Monterey No. 0 Sand (13 tests) and Banding Sand (9 tests). The main objectives of these tests was to study the effect of anisotropic consolidation, static shear stresses, and of relative density on the value of the threshold strain, γ_t, and on the rate of pore pressure buildup at cyclic strains slightly larger than the threshold. The influence of anisotropic consolidation was measured by consolidating the sand specimens, prior to cyclic testing, to stress ratios ($k_c = \bar{\sigma}_{ho}/\bar{\sigma}_{vo}$) ranging between 1.0 and 2.5, and also by running two tests where a consolidation torque, T, was applied to the specimen. In all 22 tests, $\bar{\sigma}_{ho}$ = 2 ksf. The influence of relative density, D_r, was measured by conducting tests on specimens compacted in very loose (D_r = 20%) and medium dense (D_r = 60%) conditions. On the basis of these tests it is possible to conclude the following:

(1) In isotropically consolidated (k_c = 1.0) Monterey No. 0 sand, γ_t = 0.01% for both D_r = 20% and D_r = 60%. This is consistent with previous results on this sand, obtained for the overlapping range 45% < D_r < 80%. Therefore, for Monterey No. 0 sand isotropically consolidated under $\bar{\sigma}_{ho} = \bar{\sigma}_{vo}$ = 2 ksf, γ_t = 0.01% for all relative densities between very loose (D_r = 20%) and dense (D_r = 80%).

(2) For isotropically consolidated (k_c = 1.0) Banding sand, γ_t = 0.8 to 0.9 x 10^{-2}% for both D_r = 20% and D_r = 60%. As both Banding and Monterey No. 0 sands are similar, uniform, clean quartz sands, with approximately parallel grain size distribution curves, but with the Banding sand being finer in size, this result may indicate a trend for γ_t to decrease as the grain size decreases.

(3) For both Monterey No. 0 sand and Banding sands, the pore pressure buildup after a small (n = 5) number of cycles of a cyclic strain slightly larger than γ_t, was somewhat larger for the looser (D_r = 20%) specimens as compared with the denser (D_r = 60%) specimens tested.

(4) The cyclic tests on anisotropically consolidated (k_c > 1.0) Monterey No. 0 sand and Banding sand specimens showed a similar effect of k_c on γ_t and pore pressure buildup. For both sands, the value of γ_t was unaffected by k_c, for the range $1.0 \leq k_c \leq 2.0$. In the same range of k_c = 1 to 2, and for a given D_r, the pore pressure buildup after n = 5 cycles of a cyclic shear strain slightly larger than the threshold was also about equal to the buildup measured in the isotropic case (k_c = 1.0). The behavior for the two tests conducted on Monterey No. 0 sand with k_c = 2.5 was more complex, with slightly negative pore pressures at strains immediately below γ_t = 0.01%, and

with development of positive pore pressures for strains larger than 0.01% to 0.02%. The positive pore pressures for k_c = 2.5 were either equal or smaller than those measured at the same strains for $1.0 \leq k_c \leq 2.0$. Therefore, the value $\gamma_t \approx 0.01\%$ can be used conservatively for isotropically or anisotropically consolidated Monterey No. 0 sand in loose or dense condition, and for the range $1.0 \leq k_c \leq 2.5$.

(5) Two other tests were performed on Monterey No. 0 sand specimens at $D_r \approx 20\%$ and $D_r = 60\%$, and with "k_c" = $\bar{\sigma}_{ho}/\bar{\sigma}_{vo} = 1.0$. These tests differed from the other tests in that a static torque, T, was applied during consolidation. The value of T was selected to have a mobilized angle of friction at the end of consolidation at the outer edge of the specimen similar to that mobilized in the whole specimen during the tests with $k_c = 2.0$ and T = 0. As expected, the value of γ_t and the pore pressure buildup behavior in these two tests were similar to that observed, for a comparable relative density, in specimens consolidated with T = 0 and $1.0 \leq k_c \leq 2.0$.

(6) In all tests, the cyclic axial undrained Young's modulus, E, was also obtained. This included nondestructive measurements of E at cyclic shear strains, γ_c, as low as 0.003%. Plots showing the variation of modulus versus

cyclic shear strain, and the influence of D_r and k_c on E, are presented in the report for Monterey No. 0 sand.

In summary, it has been established that, for these two sands and for the testing conditions previously described: i) γ_t is a constant characteristic of the sand for a wide range of relative densities including a very loose condition, and ii) the γ_t concept is valid for anisotropically consolidated sand, and the use of γ_t determined from isotropically consolidated specimens is either realistic or slightly conservative for the range $1.0 \leq k_c \leq 2.5$, at least for the cases studied here, in which $\bar{\sigma}_{3c} = 2$ ksf.

REFERENCES

1. Castro, G. (1969), "Liquefaction of Sands," Ph.D. Thesis, Harvard Soil Mechanics Series, No. 81, Pierce Hall, Harvard University.

2. Dobry, R. and Ladd, R.S. (1980), "Discussion of 'Soil Liquefaction and Cyclic Mobility Evaluation for Level Ground During Earthquakes' by H.B. Seed, and of 'Liquefaction Potential: Science Versus Practice' by R. Peck," Journal of Geotechnical Engineering Division, ASCE, June, Vol. 106, No. GT6, pp. 720-724.

3. Dobry, R., Powell, D.J., Yokel, F.Y. and Ladd, R.S. (1980), "Liquefaction Potential of Saturated Sand - The Stiffness Method," Proc. Seventh World Conference on Earthquake Engineering, Istanbul, Turkey, September, Vol. 3, pp. 25-32.

4. Dobry, R., Yokel, F.Y. and Ladd, R.S. (1981), "Liquefaction Potential of Overconsolidated Sands in Moderately Seismic Areas," Proc. Conf. on Earthquake and Earthquake Engineering in the Eastern U.S., Knoxville, TN, Sept., Vol. 2, pp. 643-664.

5. Dobry, R., Stokoe, K.H. II, Ladd, R.S. and Youd, T.L. (1981a), "In Situ Shear Wave Velocity Measurements to Evaluate Liquefaction Susceptibility," submitted to session on "In Situ Tests to Evaluate Liquefaction Susceptibility," ASCE National Convention, St. Louis, Missouri, October.

6. Dobry, R., Ladd, R.S., Yokel, F.Y., Chung, R.M. and Powell, D.J. (1982), "Prediction of Pore Pressure Buildup and Liquefaction of Sands During Earthquakes by the Cyclic Strain Method," National Bureau of Standards Building Science Series, No. 138, July.

7. Finn, W.D.L., Lee, K.W., Maartman, C.H. and Lo, R. (1978), "Cyclic Pore Pressures under Anisotropic Conditions," Proceedings of Spec. Conference on Earthquake Engineering and Soil Dynamics, ASCE, Vol. 1, pp. 457-471, Pasadena, California.

8. Geotechnical Engineers Inc. (1982), "Liquefaction Induced by Cyclic Loading," Project No. 80696 Report to the National Science Foundation, March.

9. Ishihara, K. (1981), "Pore Water Pressure Rises During Earthquakes," Proc. Int. Conf. on Recent Advances in Geotechnical Earthquake Engineering and Soil Dynamics, St. Louis, MI, May, Vol. III, pp. 1-4.

10. Ladd, R.S. (1978), "Preparing Test Specimens Using Under Compaction," Geotechnical Testing Journal, ASTM, Vol. 1, No. 1, March, pp. 16-23.

11. Lee, K.L. and Seed, H.B. (1967) "Dynamic Strength of Anisotropically Consolidated Sand," Journal of the Soil Mechanics and Foundation Division, ASCE, Vol. 93, No. SM5, pp. 169-190.

12. Mulilis, J.P., Chan, C.K. and Seed, H.B. (1975), "The Effects of Method of Sample Preparation on the Cyclic Stress-Strain Behavior of Sands," Report No. EERC 75-18, Earthquake Engineering Research Center, University of California, Berkeley, July.

13. Pyke, R.M., Chan, C.K. and Seed, H.B. (1974), "Settlement and Liquefaction of Sands under Multi-Directional Shaking," Report No. EERC 74-2, Earthquake Engineering Research Center, University of California, Berkeley, February.

14. Seed, H.B., Lee, K.L., Idriss, I.M. and Makdisi, F.I. (1973), "Analysis of Slides in the San Fernando Dams During the Earthquake of February 9th, 1971", Report No. EERC 73-2, University of California, Berkeley.

15. Seed, H.B., Mori, K. and Chan, C.K. (1977), "Influence of Seismic History on Liquefaction of Sands," Journal of the Geotechnical Engineering Division, ASCE, Vol. 103, No. GT4, Proc. Paper 12841, April, pp. 246-270.

16. Thomas, G.E., Dyvik, R., Dobry, R. and Ladd, R.S. (1982), "Experimental Study of the Cyclic Constitutive Relation of Saturated Sands During Undrained Loading," Report No. CE 82-1, Department of Civil Engineering, Rensselaer Polytechnic Institute, Troy, N.Y., February.

TABLE 1

INDEX PROPERTIES FOR MONTEREY NO.0 SAND AND BANDING SAND

	MONTEREY NO. 0 SAND	BANDING SAND
Specific Gravity	2.65	2.66
Particle Size Distribution Data		
D_{50}, mm	0.36	0.19
C_c(1)	0.9	0.9
C_u(2)	1.5	1.4
Dry Unit Weight Data		
Maximum, pcf	105.7	106
Minimum, pcf	80.3	90

(1) $C_c = (D_{30})^2/(D_{60} \times D_{10})$ (2) $C_u = D_{60}/D_{10}$

TABLE 2a

TESTS ON MONTEREY NO. 0 SAND

D_{rf}(%)	B Parameter (%)	$\bar{\sigma}_{ho}$(ksf)	$k_c = \bar{\sigma}_{vo}/\bar{\sigma}_{ho}$	T (in-lb) Torque
29.0	98.5	2.0	1.0	7.28
29.9	97.2	2.0	1.0	0.0
28.9	98.9	2.0	1.0	0.0
27.1	98.0	2.0	1.5	0.0
20.4	98.2	2.0	2.0	0.0
22.5	97.9	2.0	2.5	0.0
62.5	97.6	2.0	1.0	7.28
61.5	99.8	2.0	1.0	0.0
68.5	98.2	2.0	1.0	0.0
60.6	98.6	2.0	1.5	0.0
61.9	97.5	2.0	2.0	0.0
56.6	99.6	2.0	2.0	0.0
62.1	97.5	2.0	2.5	0.0

Specimen Size:

Height = 4.0 in

Diameter = 2.0 in

Table 2b

TESTS ON BANDING SAND

D_{rf}(%)	B (%) Parameters	$\bar{\sigma}_{ho}$(ksf)	$k_c = \bar{\sigma}_{vo}/\bar{\sigma}_{ho}$	T (in-lb) Torque
23.1	98.3	2.0	1.0	0.0
22.7	99.2	2.0	1.0	0.0
26.7	99.4	2.0	1.0	0.0
26.8	97.7	2.0	2.0	0.0
61.7	97.0	2.0	1.0	0.0
63.5	97.0	2.0	1.0	0.0
60.7	97.6	2.0	1.0	0.0
61.2	98.8	2.0	2.0	0.0
62.3	97.0	2.0	2.0	0.0

Specimen Size:

Height = 4.0 in

Diameter = 2.0 in

Figure 1 RPI Cyclic Axial/Torsional Triaxial Soil Test Equipment

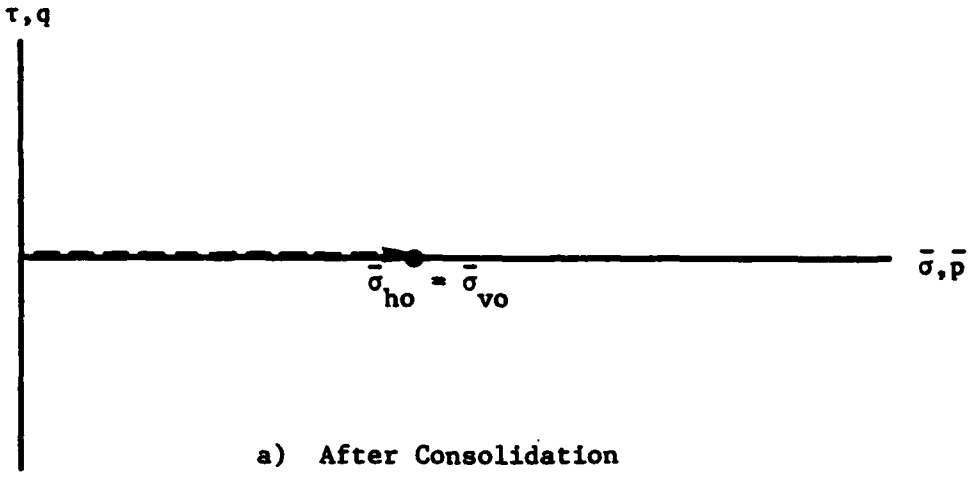

a) After Consolidation

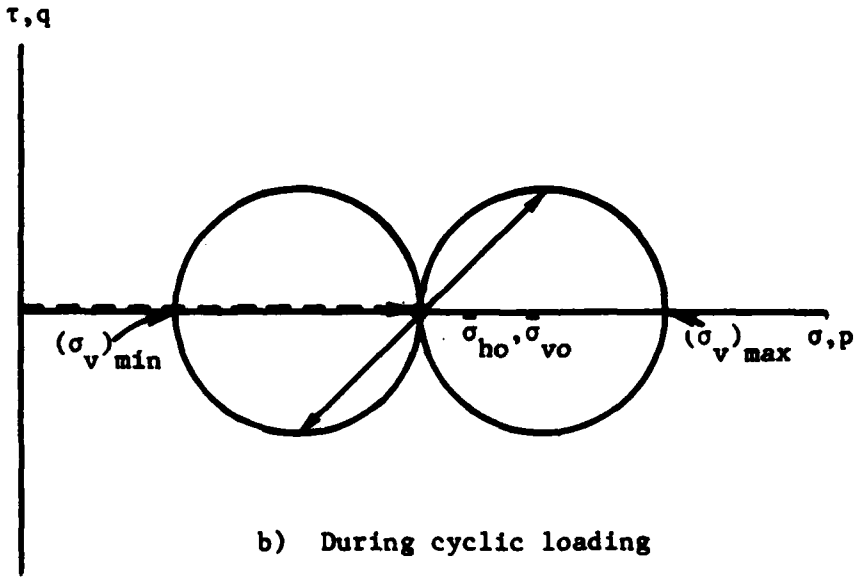

b) During cyclic loading

Figure 2 Mohr Circles and Stress Path for Isotropically Consolidated Specimens ($k_c = \bar{\sigma}_{vo}/\bar{\sigma}_{ho} = 1.0$, T = 0)

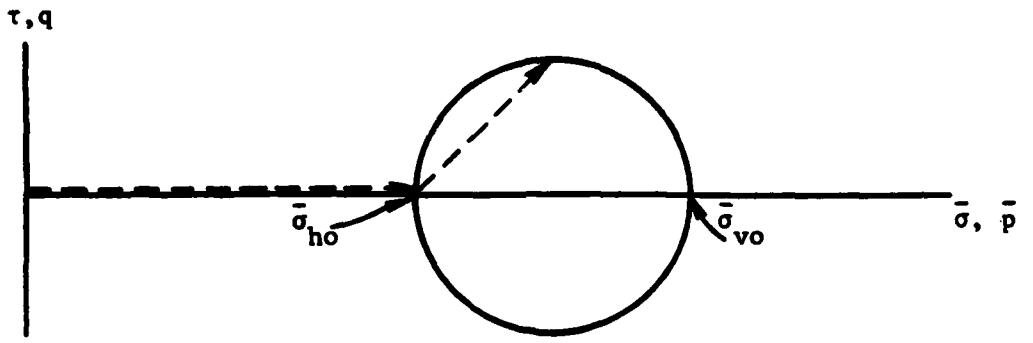

a) After Consolidation

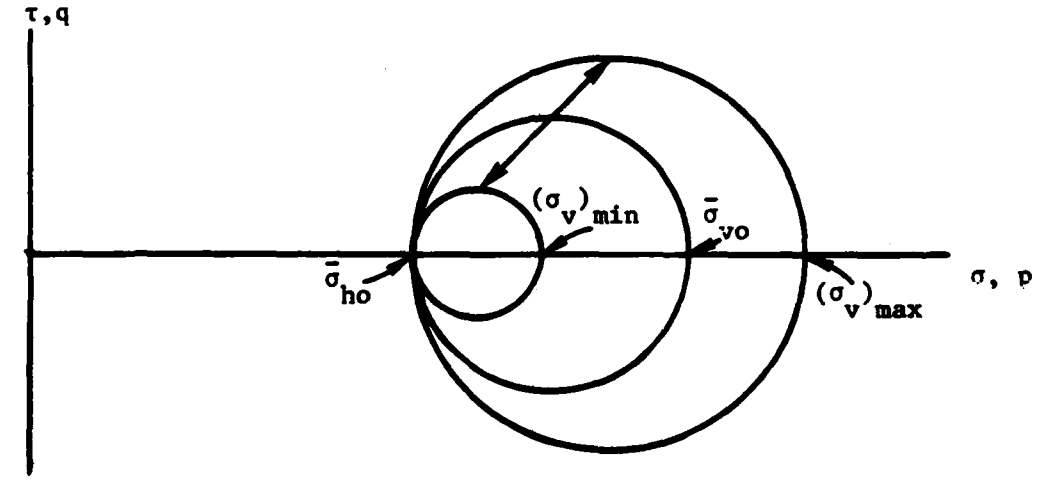

b) During Cyclic Loading with Incomplete Stress Reversal

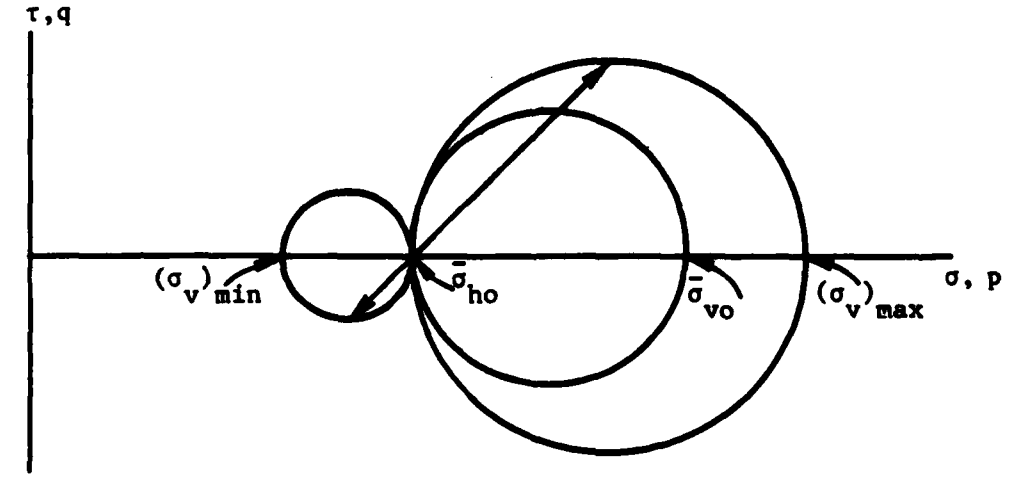

c) During Cyclic Loading with Complete Stress Reversal

Figure 3 Mohr Circles and Stress Paths for Anisotropically Consolidated Specimens ($k_c = \bar{\sigma}_{vo}/\bar{\sigma}_{ho} > 1.0$, T = 0)

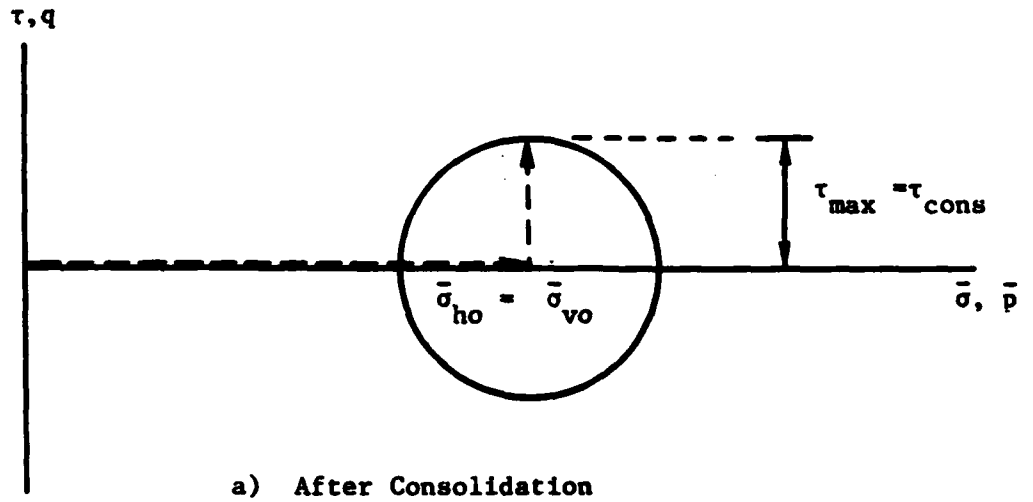

a) After Consolidation

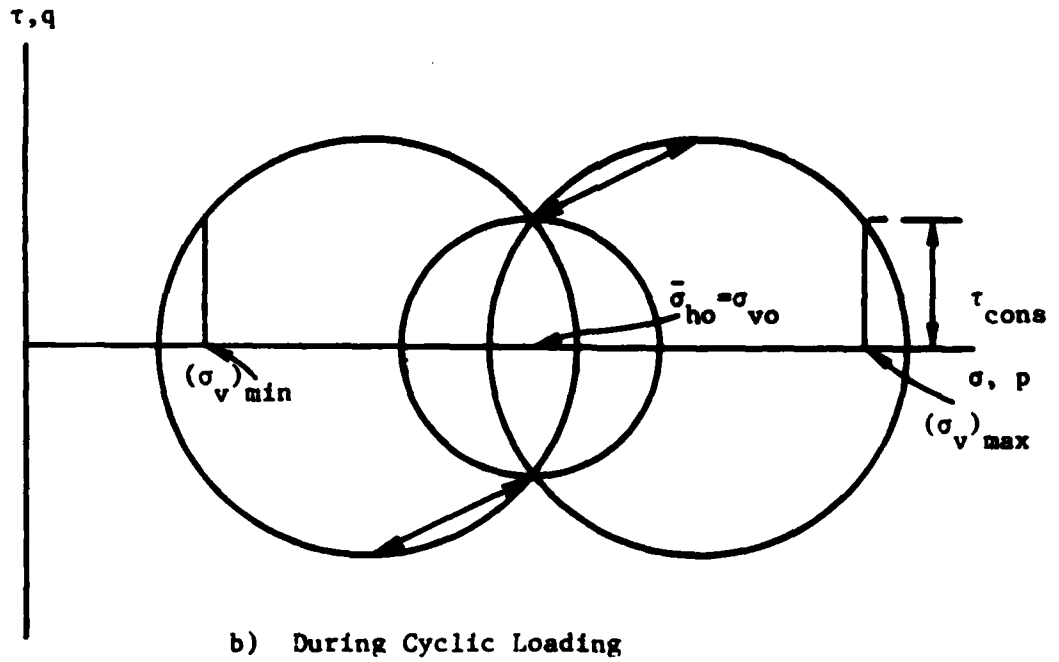

b) During Cyclic Loading

Figure 4 Mohr Circles and Stress Paths at the Outer Edge of Specimen for "Isotropically Consolidated" Specimens with a Torque Applied During Second Consolidation Stage ($k_c = \bar{\sigma}_{vo}/\bar{\sigma}_{ho} = 1.0$, $T \neq 0$)

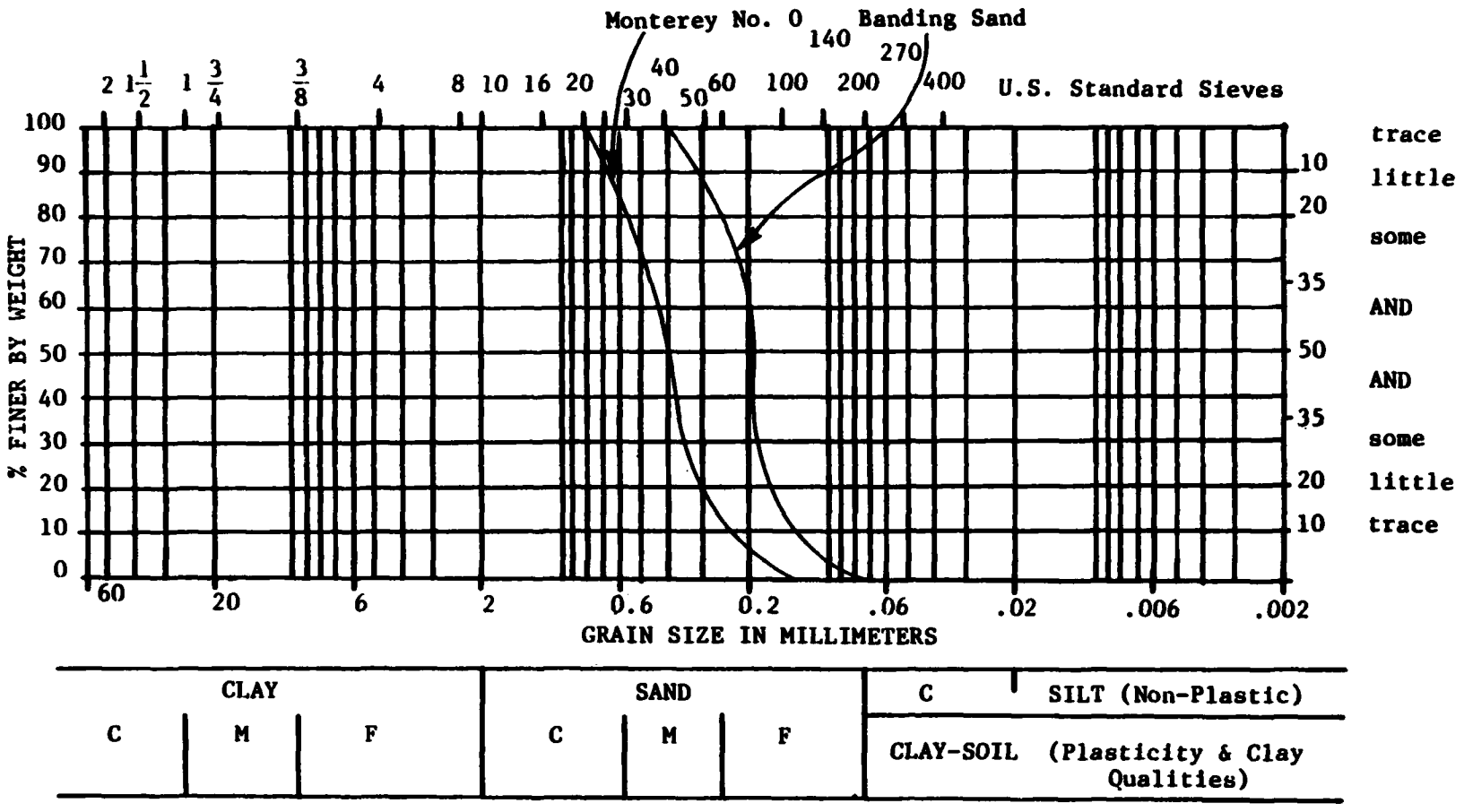

Figure 5 Grain Size Distributions of Monterey No. 0 and Banding Sand

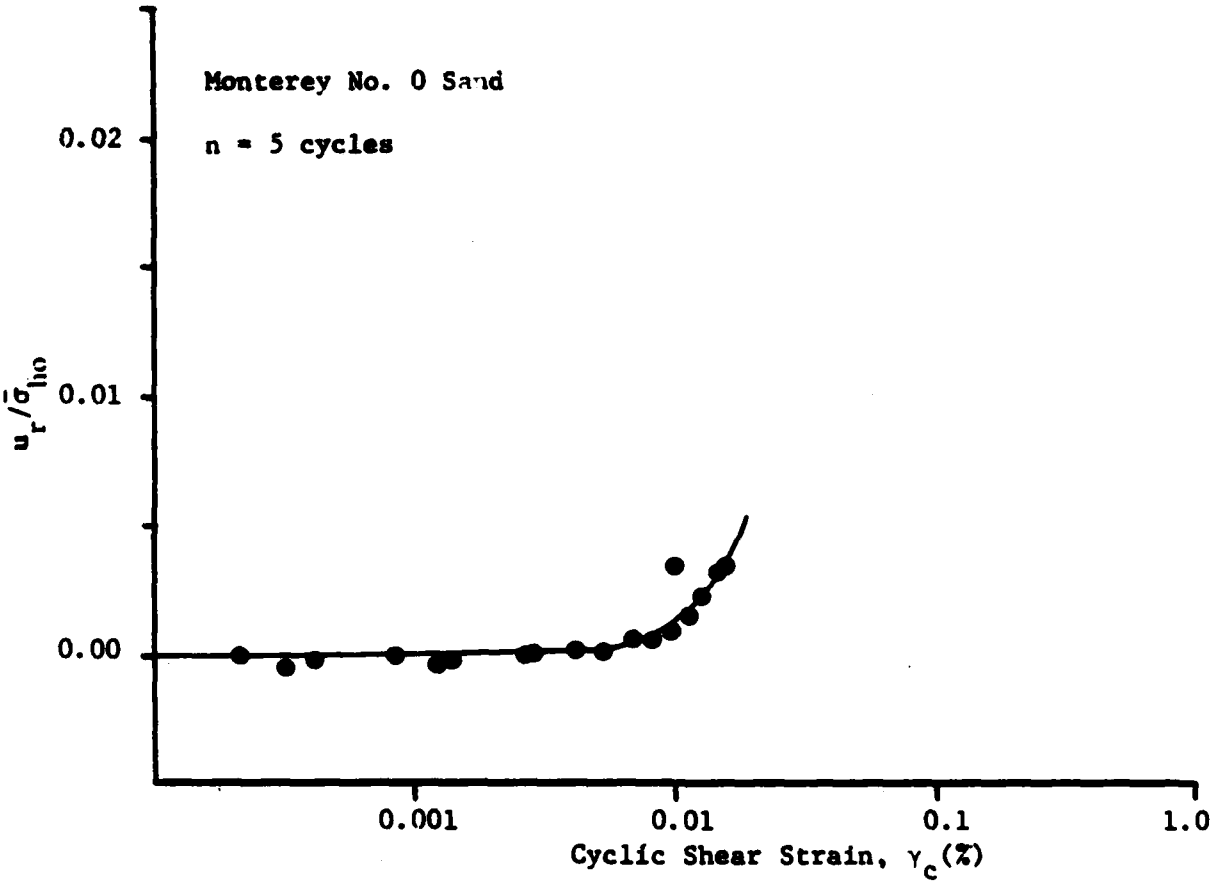

Figure 6 Normalized Residual Pore Pressure After 5 Cycles (D_{rf} = 60%, k_c = 1.0, T = 0)

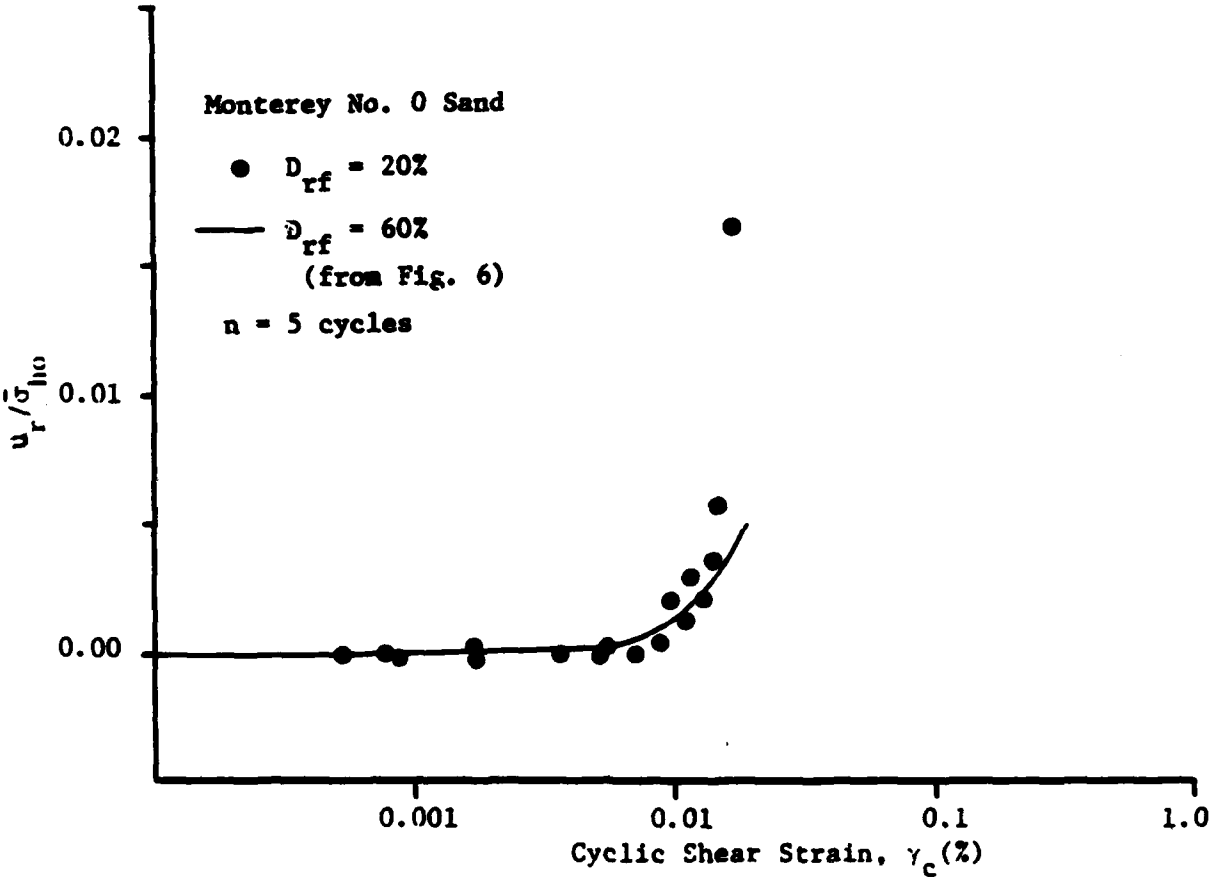

Figure 7 Effect of Relative Density on the Threshold Shear Strain (k_c = 1.0, T = 0)

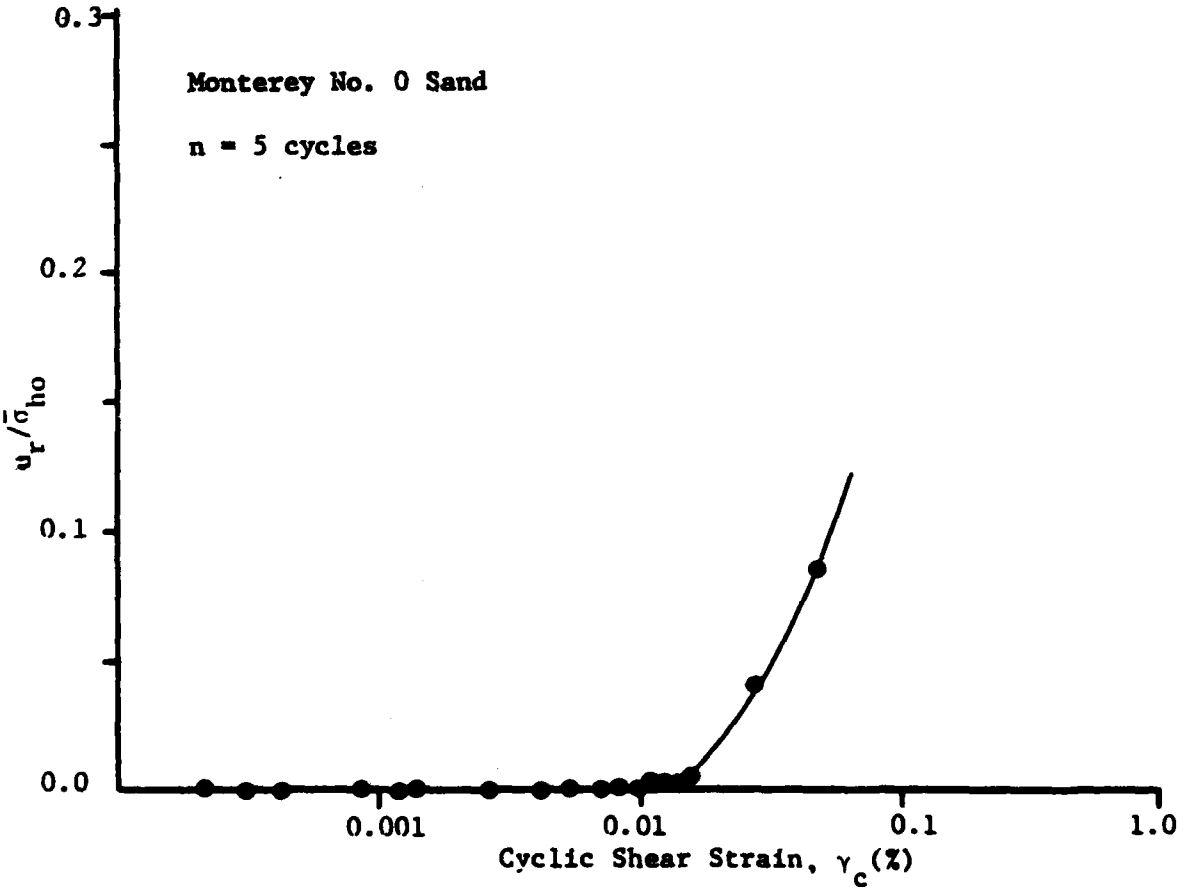

Figure 8 Normalized Residual Pore Pressure after 5 Cycles (D_{rf} = 60%, k_c = 1.0, T = 0)

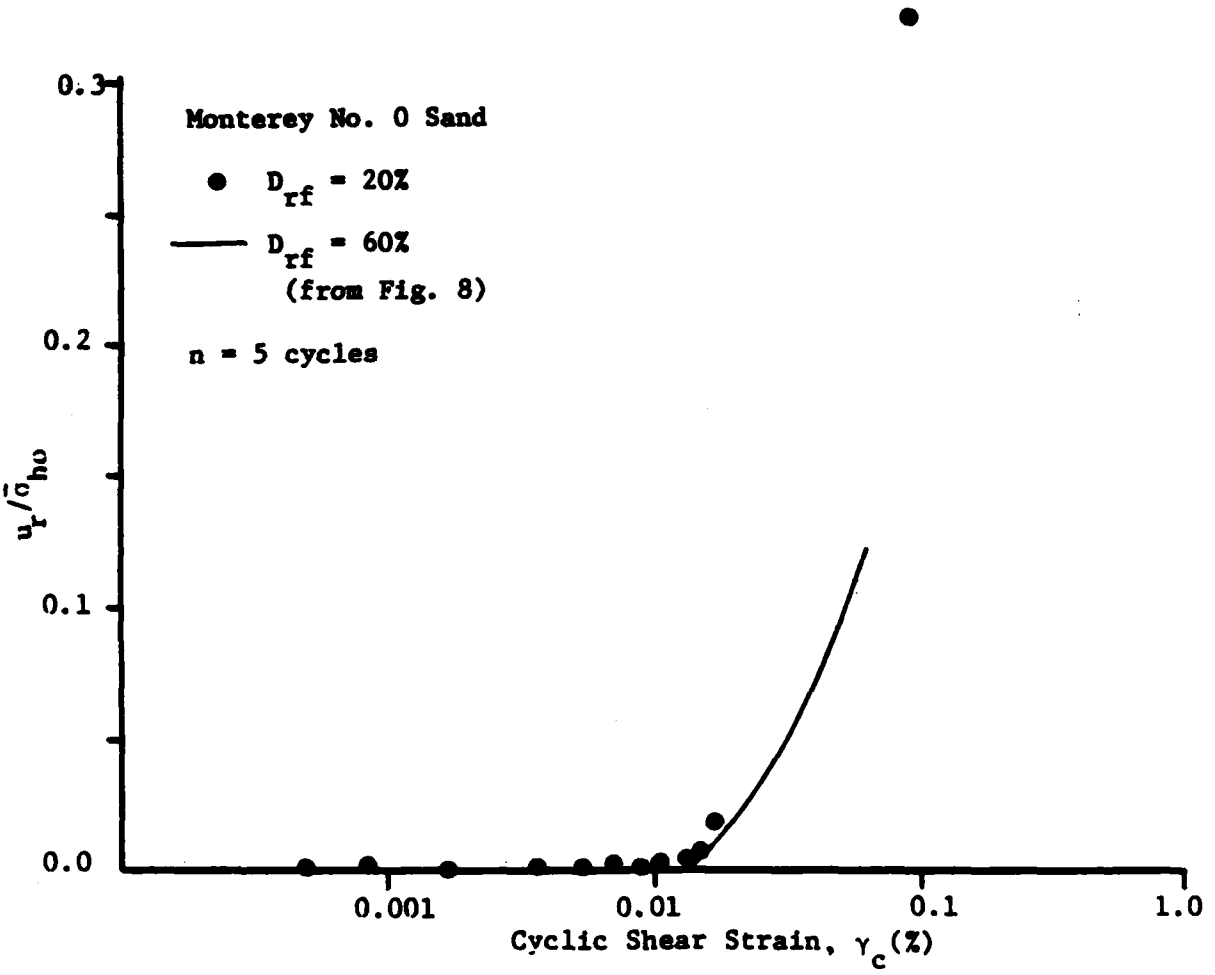

Figure 9 Effect of Relative Density on the Normalized Residual Pore Pressure after 5 Cycles (k_c = 1.0, T = 0)

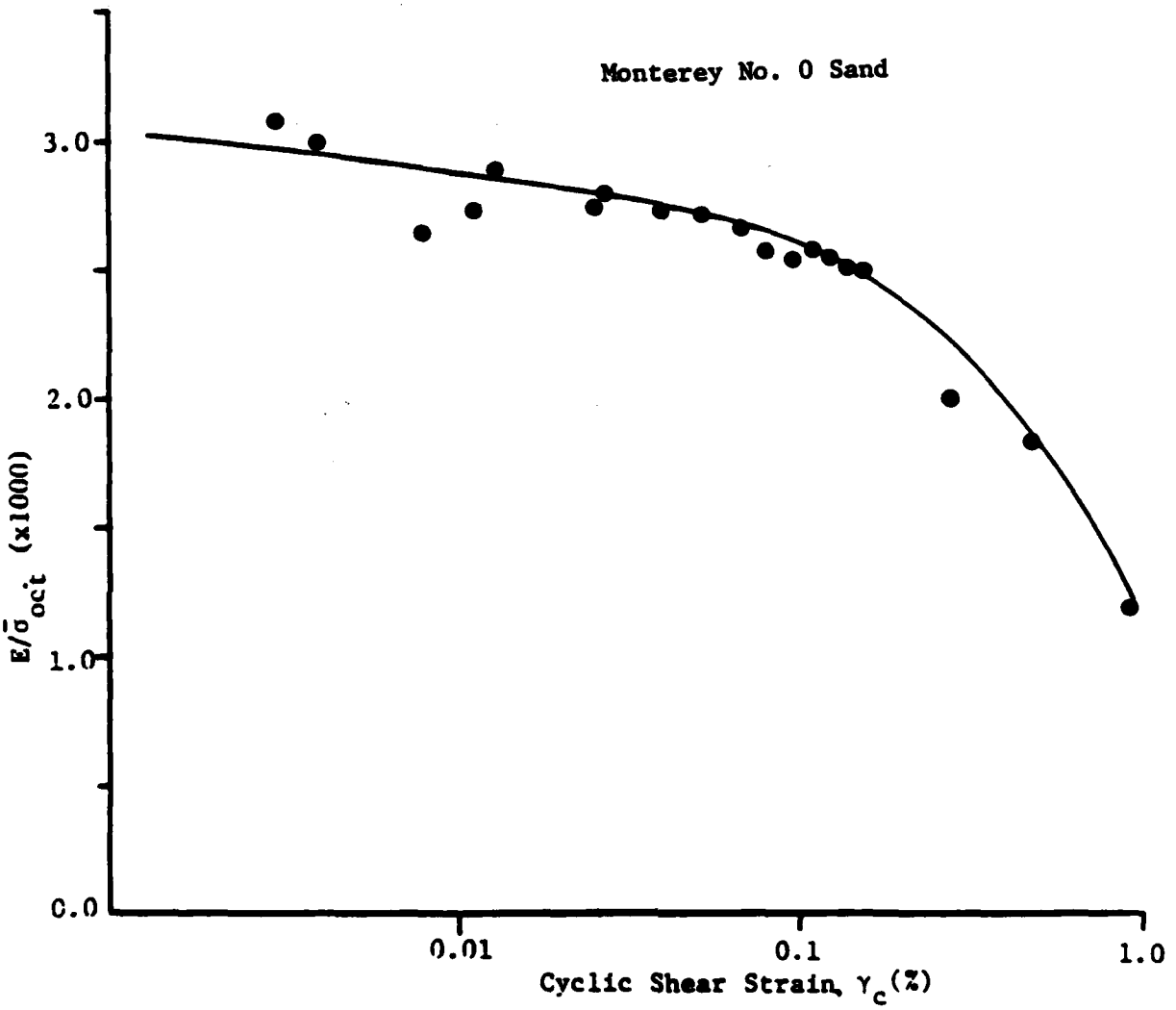

Figure 10 Normalized Young's Modulus for D_{rf} = 60%
(k_c = 1.0, T = 0)

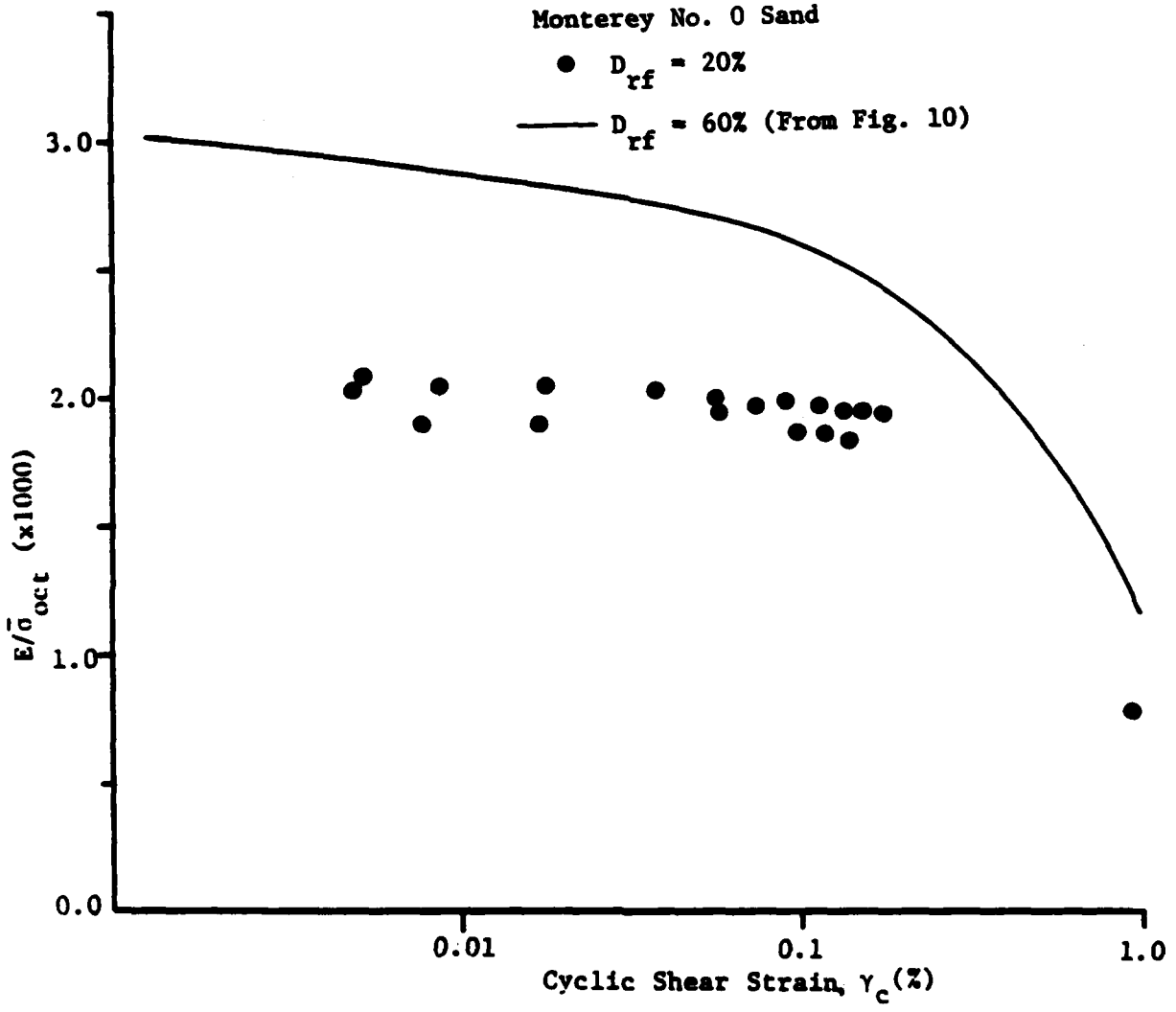

Figure 11 Effect of Relative Density on Normalized Young's Modulus (k_c = 1.0, T = 0)

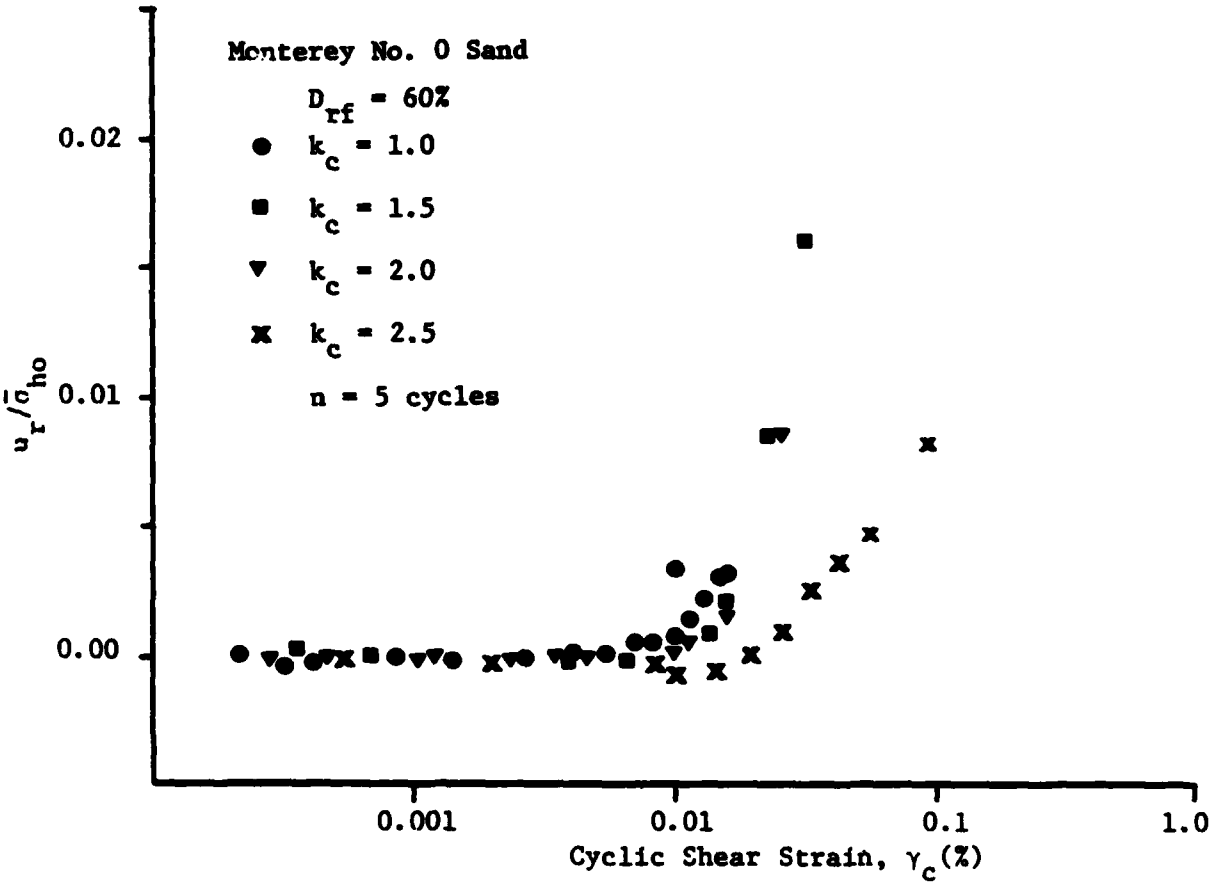

Figure 12 Effect of Anisotropic Consolidation on Threshold Shear Strain (D_{rf} = 60%, T = 0)

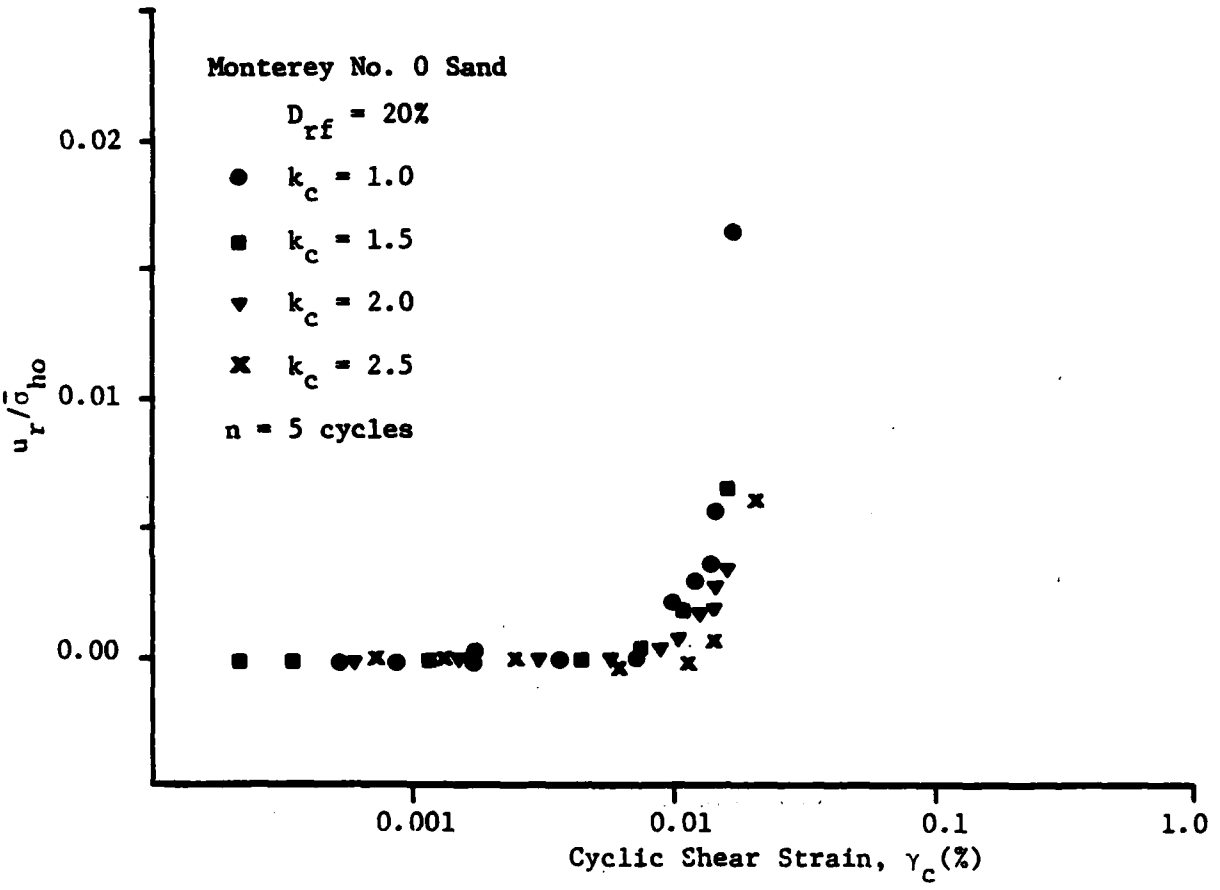

Figure 13 Effect of Anisotropic Consolidation on Threshold Shear Strain (D_{rf} ≅ 20%, T = 0)

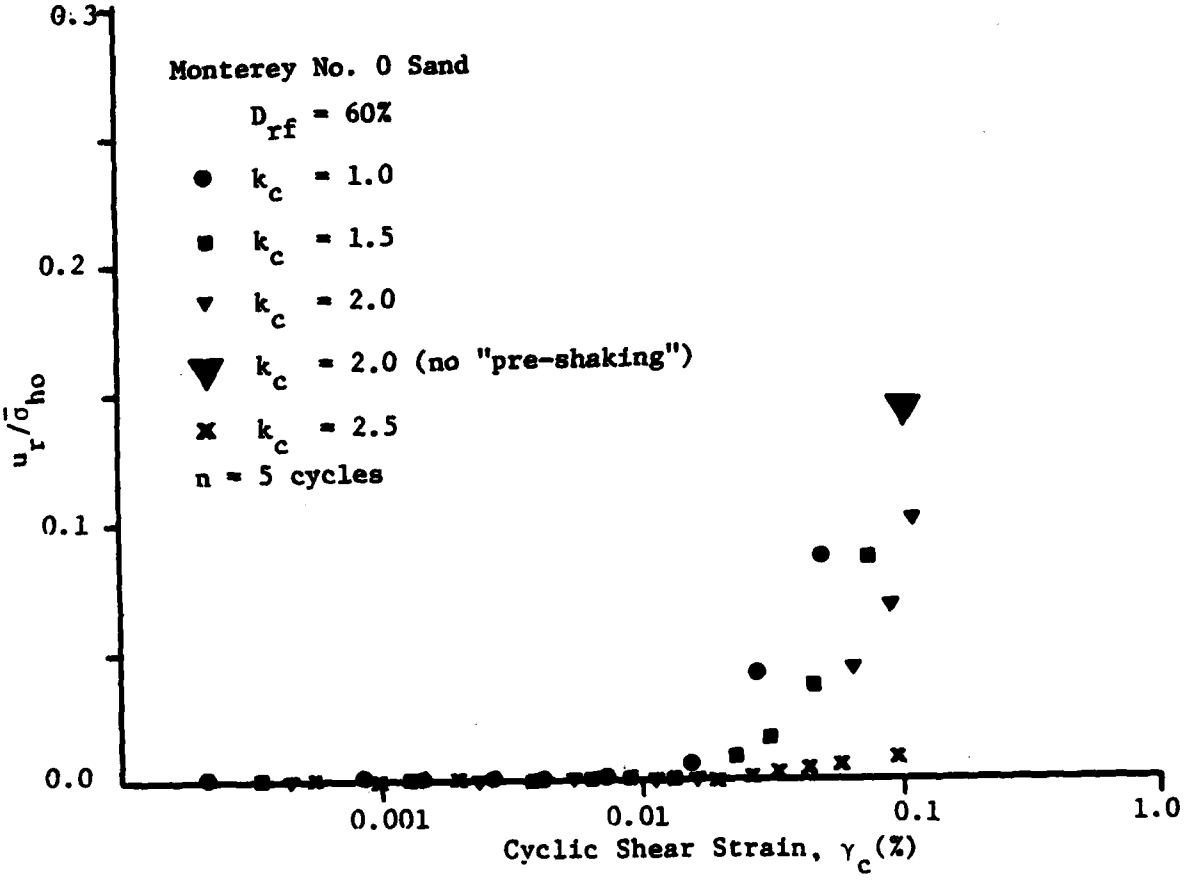

Figure 14 Effect of Anisotropic Consolidation on the Normalized Residual Pore Pressure After 5 Cycles (D_{rf} = 60%, T = 0)

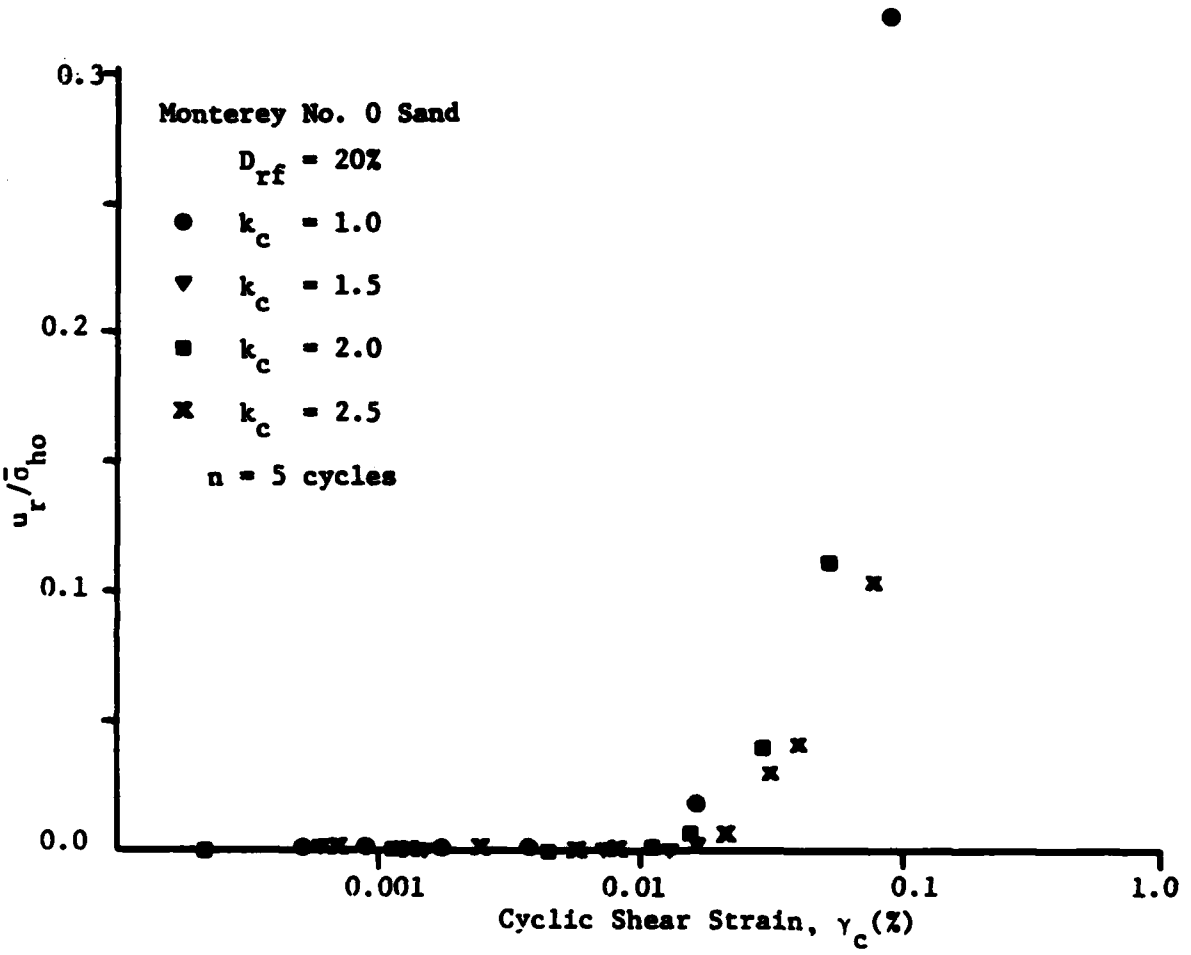

Figure 15 Effect of Anisotropic Consolidation Shear Stresses on the Normalized Residual Pore Pressure After 5 Cycles (D_{rf} = 20%, T = 0)

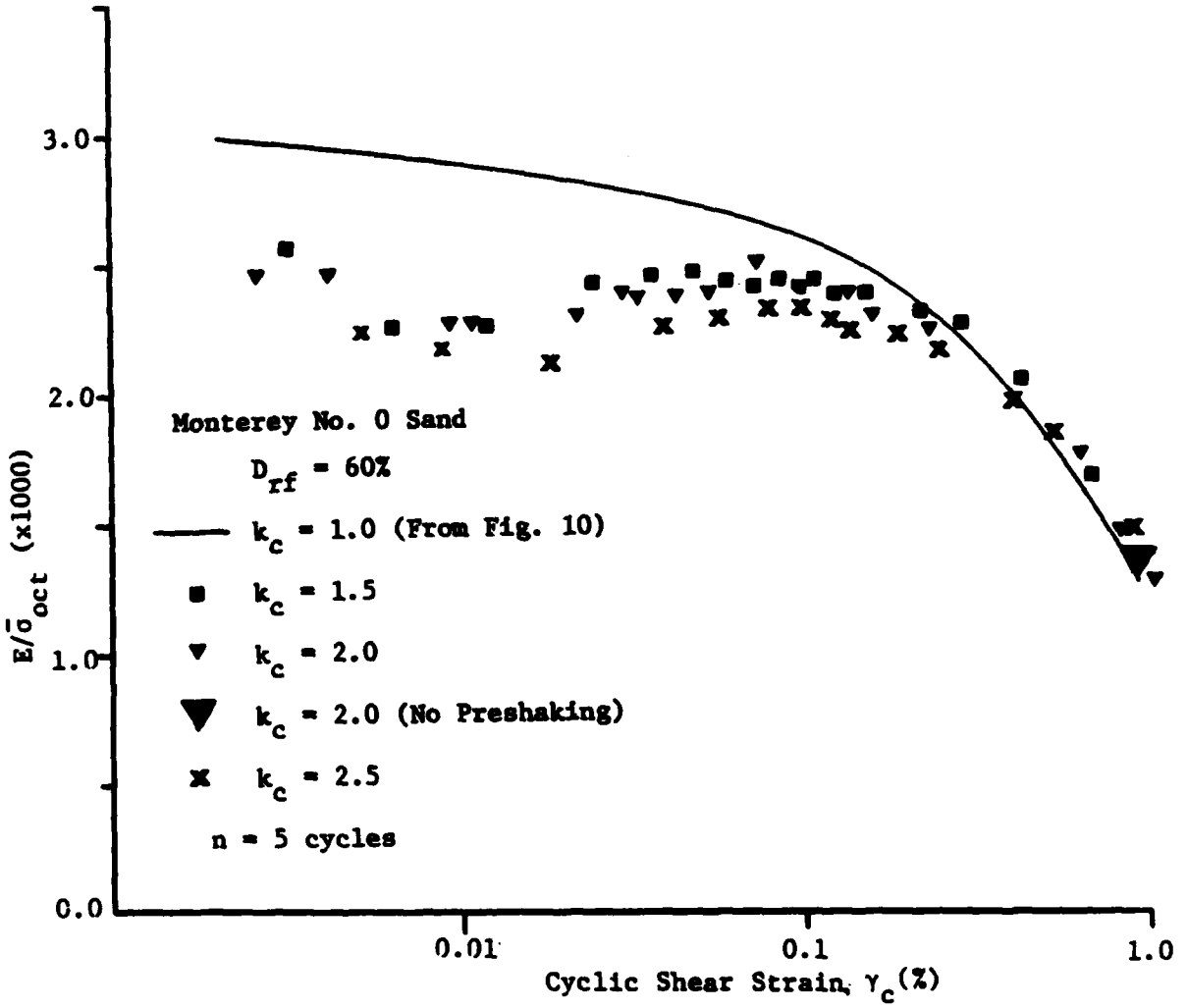

Figure 16 Effect of Anisotropic Consolidation on Normalized Young's Modulus (D_{rf} = 60%, T = 0)

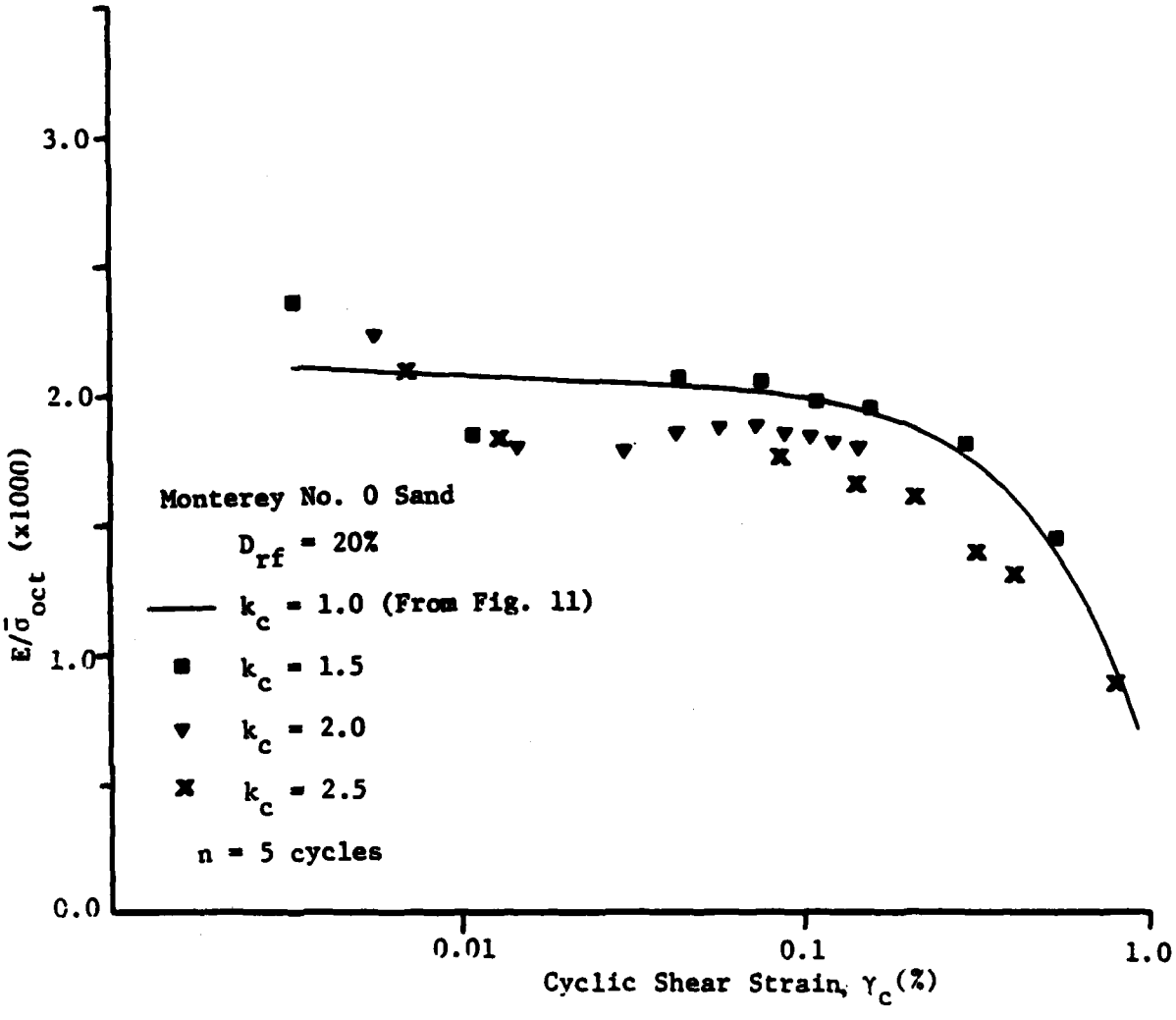

Figure 17 Effect of Anisotropic Consolidation on Normalized Young's Modulus (D_{rf} = 20%, T = 0)

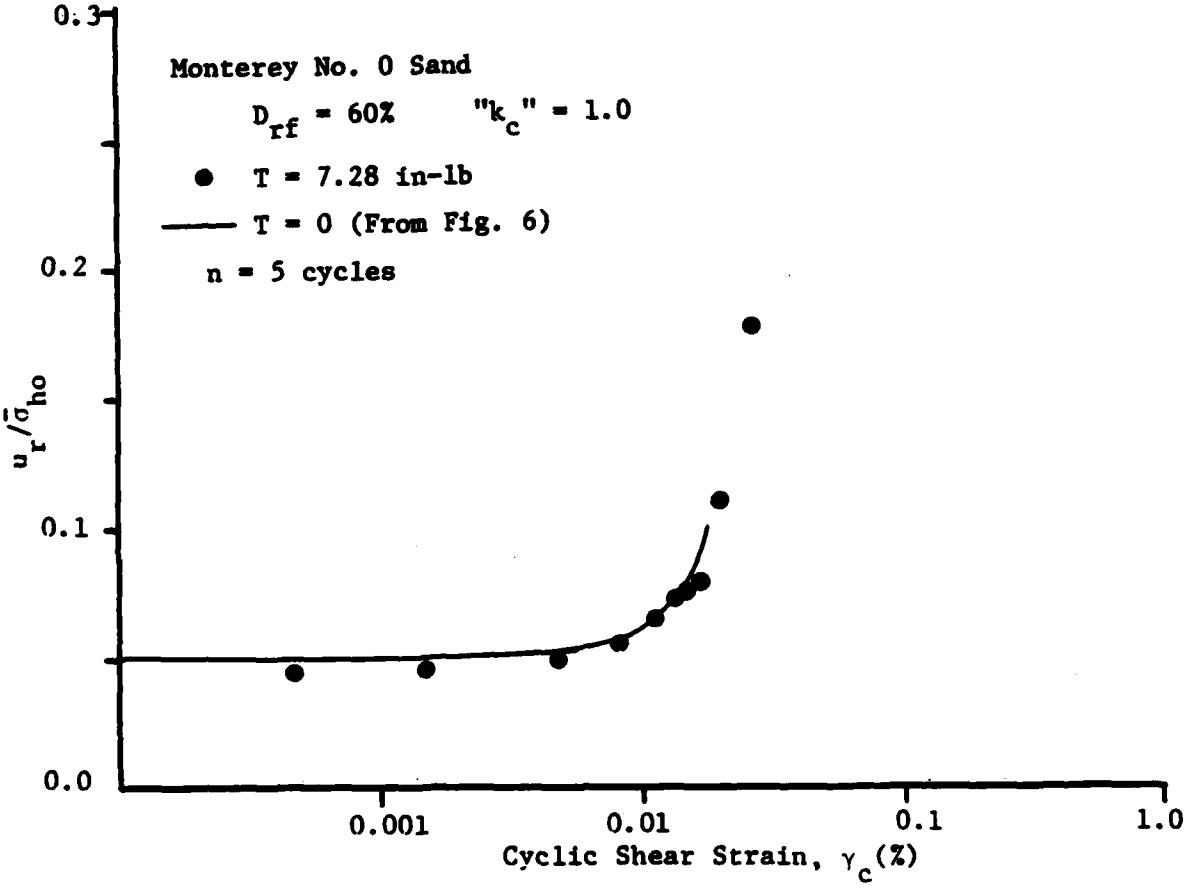

Figure 18 Effect of Consolidation Torque on the Threshold Shear Strain (D_{rf} = 60%, "k_c" = 1.0)

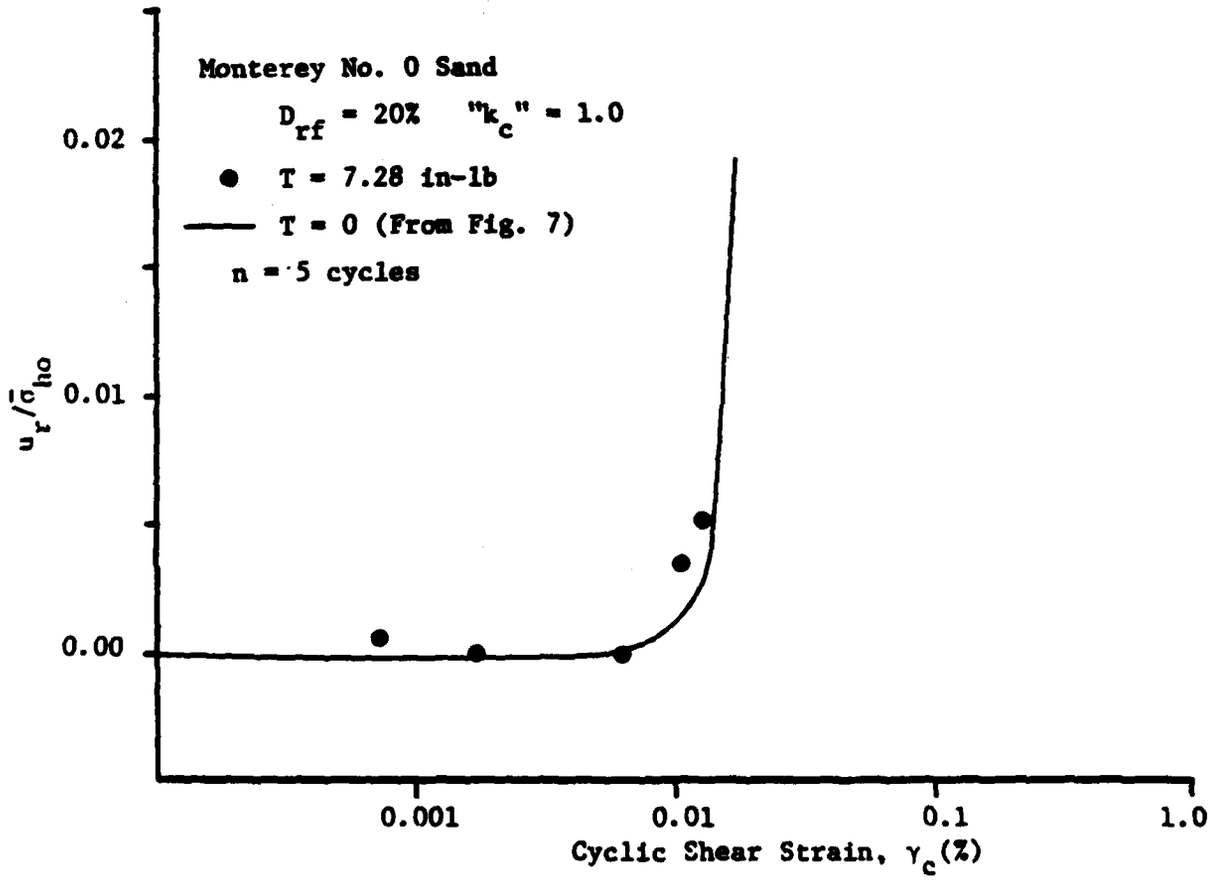

Figure 19 Effect on Consolidation Torque on the Threshold Shear Strain (D_{rf} = 20%, "k_c" = 1.0)

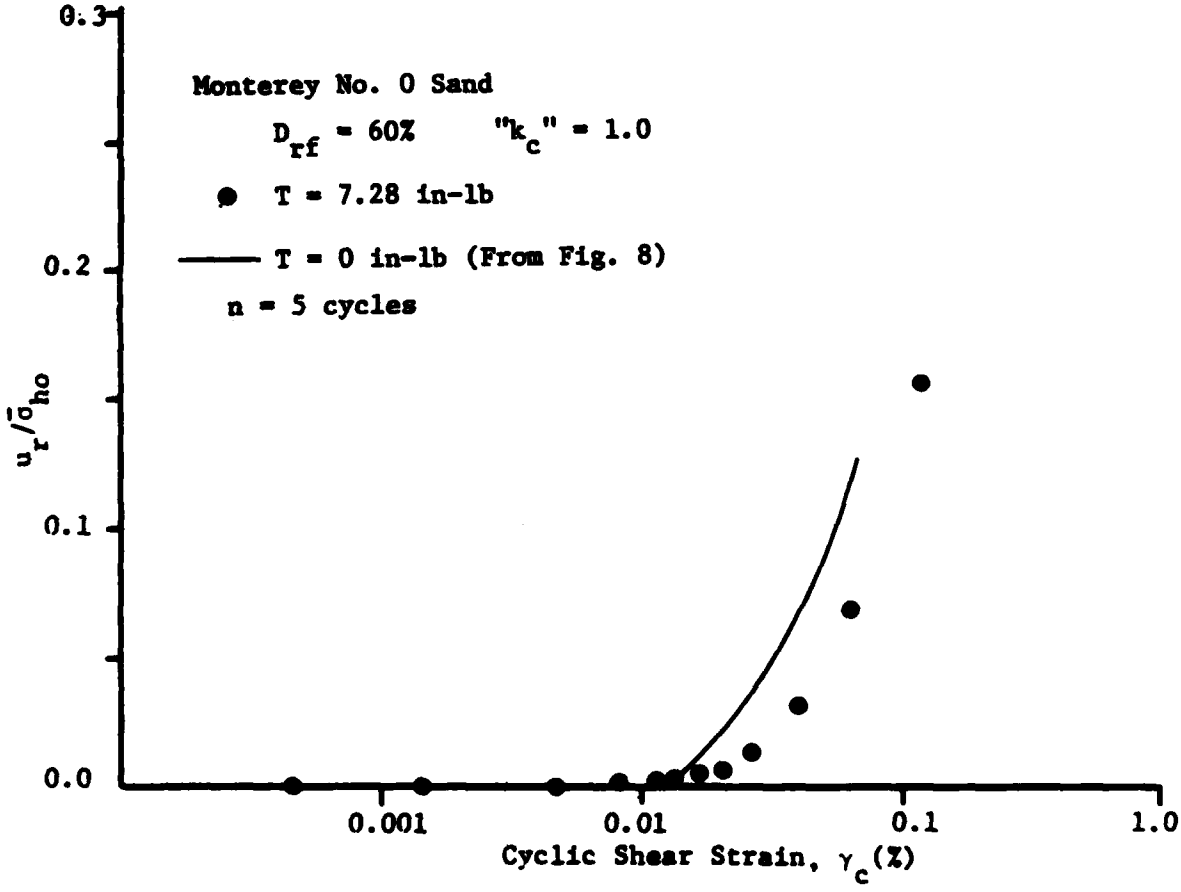

Figure 20 Effect of Consolidation Torque on the Normalized Residual Pore Pressure after 5 Cycles (D_{rf} = 60%, "k_c" = 1.0)

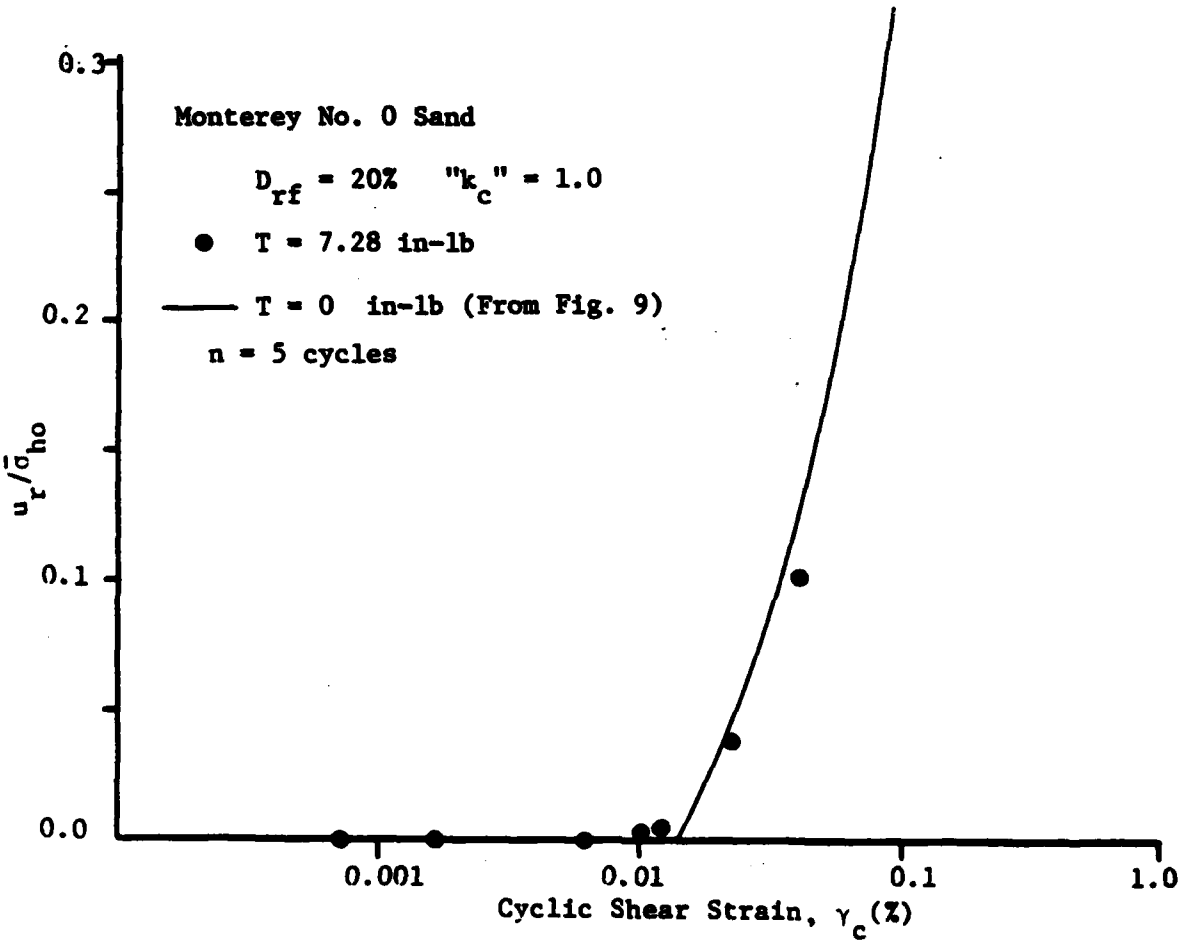

Figure 21 Effect of Consolidation Torque on the Normalized Residual Pore Pressure After 5 Cycles (D_{rf} = 20%, "k_c" = 1.0)

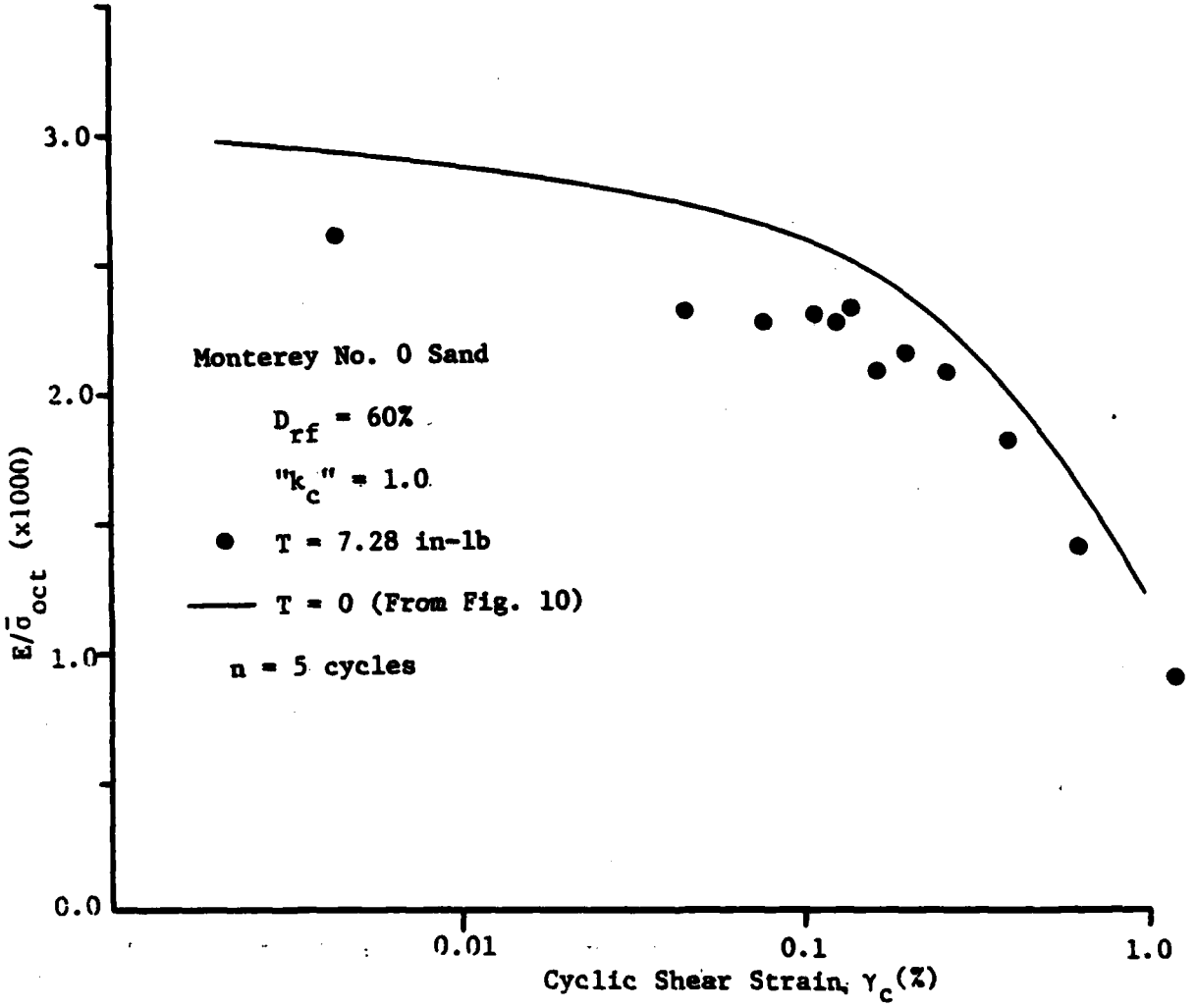

Figure 22 Effect of Consolidation Torque on Normalized Young's Modulus for D_{rf} = 60% (D_{rf} ≈ 60%, "k_c" = 1.0)

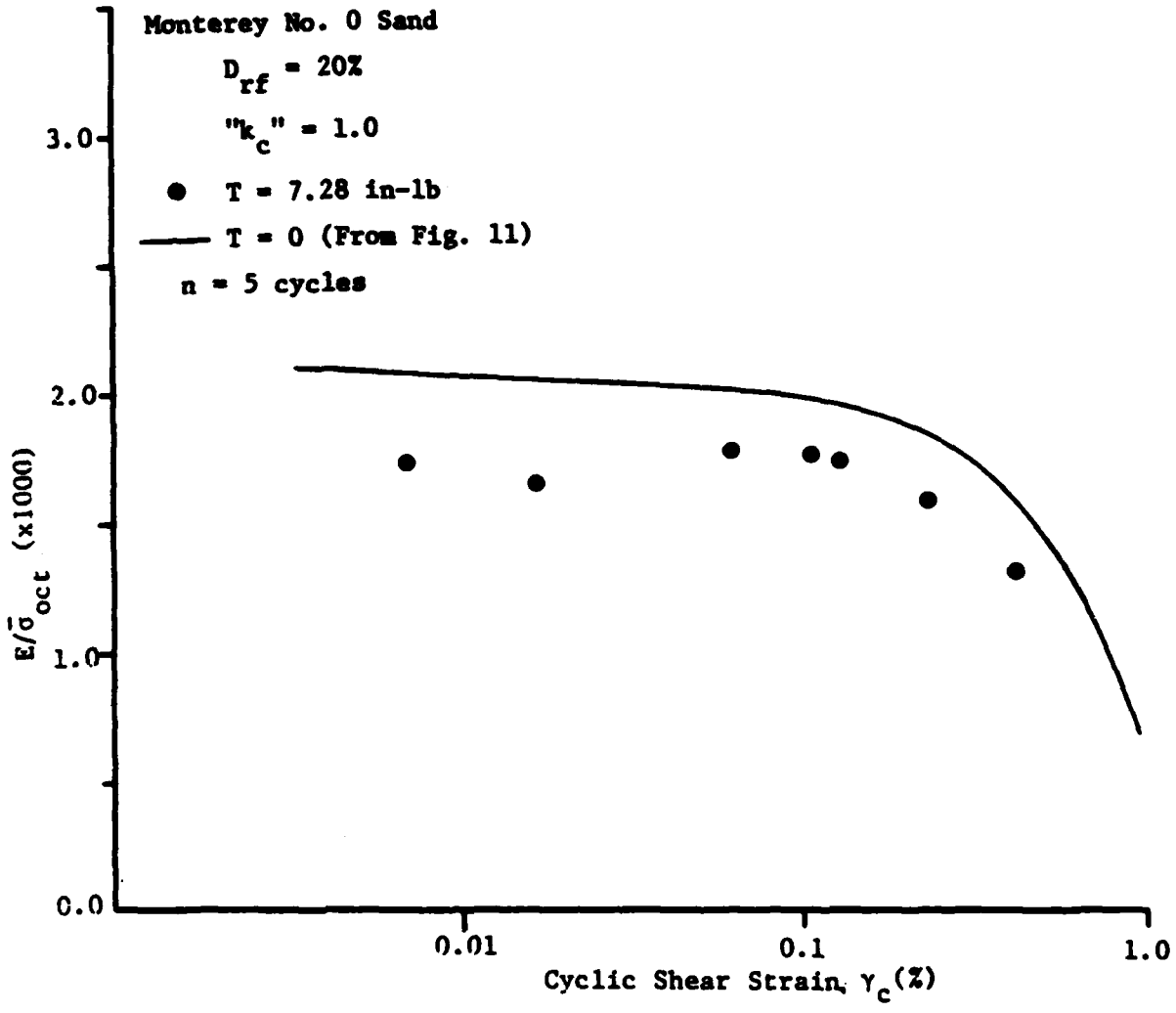

Figure 23 Effect of Consolidation Torque on Normalized Young's Modulus for D_{rf} = 20% (D_{rf} = 20%, "k_c" = 1.0)

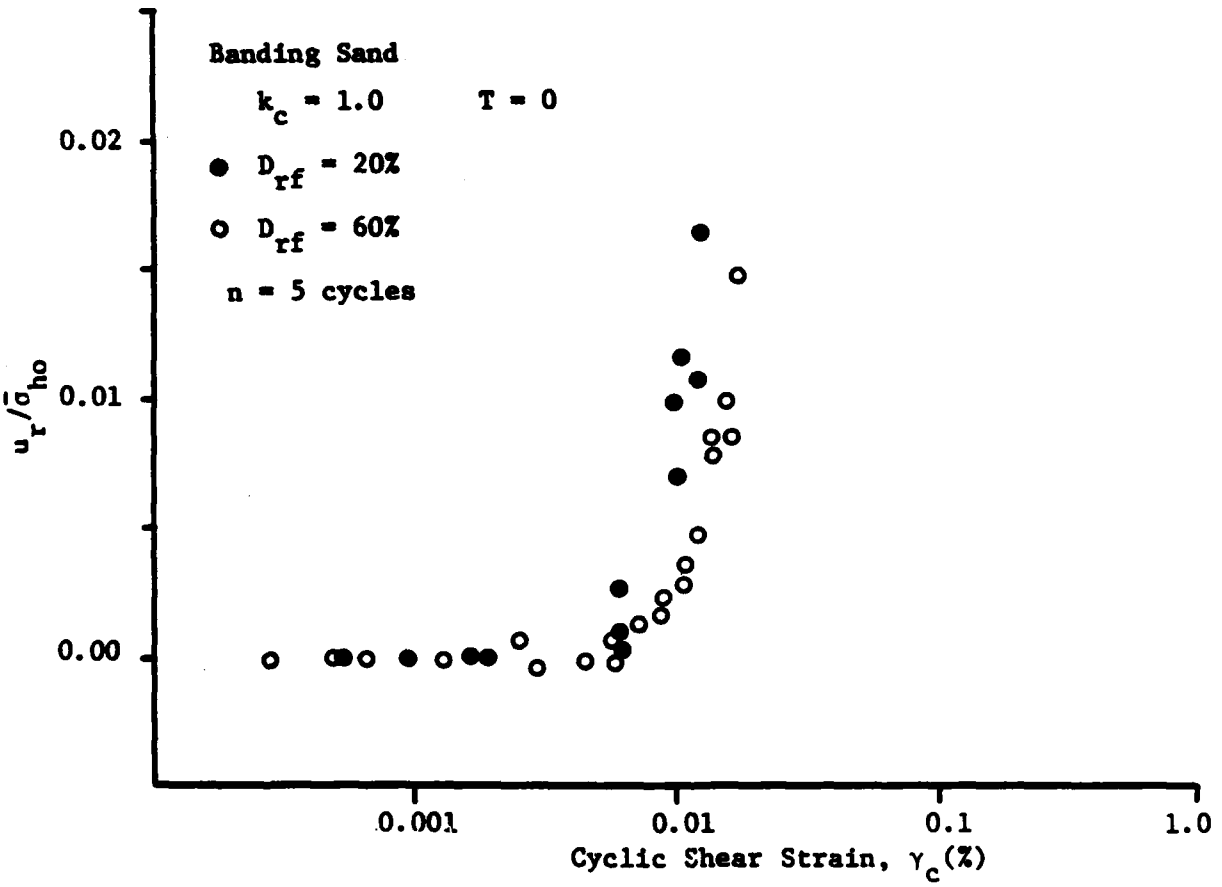

Figure 24 Effect of Relative Density on Threshold Shear Strain (k_c = 1.0, T = 0)

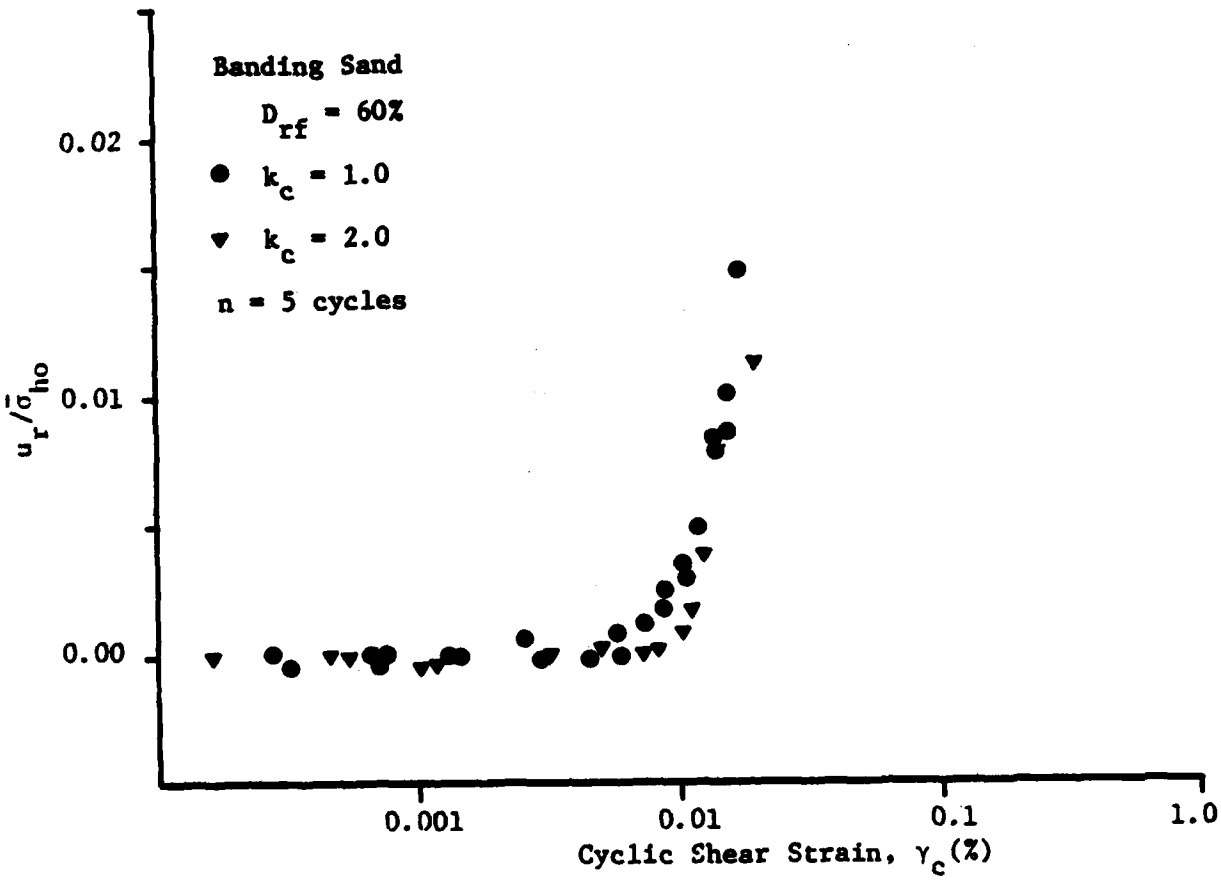

Figure 25 Effect of Anisotropic Consolidation on Threshold Shear Strain (D_{rf} = 60%, T = 0)

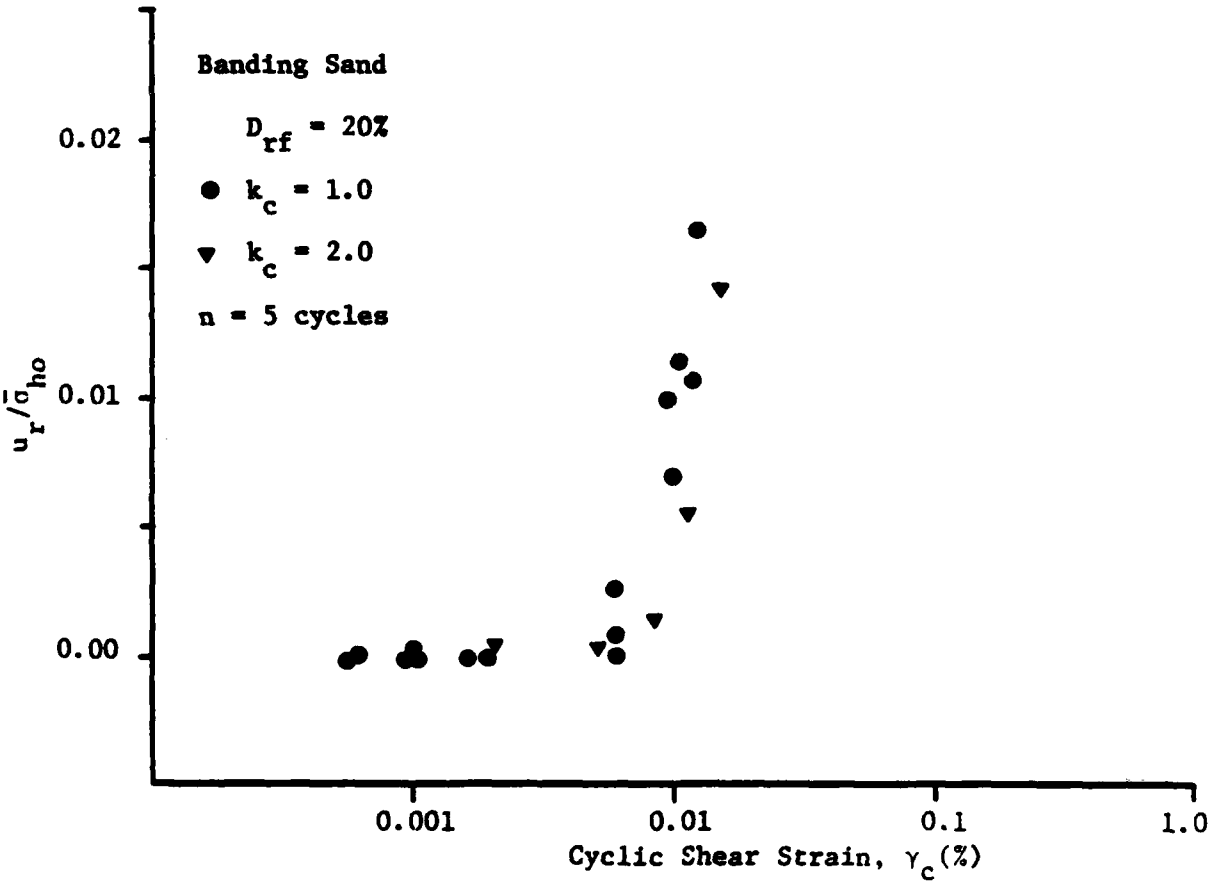

Figure 26 Effect of Anisotropic Consolidation on Threshold Shear Strain (D_{rf} = 20%, T = 0)

APPENDIX A

MEASUREMENT SYSTEM SPECIFICATIONS AND CALIBRATIONS

The soil response during the undrained cyclic triaxial tests was evaluated from simultaneous time history records of load, axial and/or angular sample displacements, and excess pore water pressure. For the test series reported herein, the measurement system used was composed of transducers, signal conditioning equipment, recorders, and connecting cables. The performance and accuracy of this electromechanical measurement system depends on the use and interaction of the complete system.

Characteristic specifications for the transducers and for the complete measuring system are shown in Table A1 and Table A2, respectively. The meaning and rationale for these specifications is detailed in this appendix and a summary of Table A2 was presented on page 8 of the report.

The fundamental specification for a transducer is its operating or linear range. A range is described by the upper and lower input values the transducer is intended to measure. The nominal linear range for each transducer, as reported in Table A1, is the range within which the transducer has an output of specified linearity, as explained below.

The transducers were all calibrated in four ranges, with the full scale output from the conditioner (± 10.000 volts) generally being set at 100%, 50%, 20% and 10% of the nominal linear range for that transducer. The transducers were calibrated for each range by zeroing the transducer output and then applying a full scale static

input for that range to the transducer and adjusting the conditioner output to provide + 10.000 volts. A full scale input in the other direction was then applied (except for the pressure transducer), and the output was adjusted to -10.000 volts. Since only low frequency tests were conducted, static calibration methods were used. The axial load, torque, and angular displacement transducers were calibrated by MTS using their calibration standards. The axial displacement transducer was calibrated and checked on a Shaevitz LVDT calibrator stand and an Instron Biaxial Extensometer Calibration fixture with vernier scales readable to 0.0001 inch and 0.001 inch, respectively. The pore pressure transducer was calibrated using a 36 inch mercury well type manometer accurate to ± 2% full scale and a 400 psi pressure gauge with a maximum nonlinearity and hysteresis of 0.1%.

The linearity of a transducer refers to the maximum deviation of any calibration point from a straight line during any one calibration cycle over a specified range. The hysteresis of the transducer refers to the maximum difference in output at any given input value, within the specified range, when the value is approached first with increasing and then with decreasing inputs. Linearity and hysteresis are expressed in percent of full scale output for the specified range and their combined values are indicative of the characteristic error of the system.

The linear range of any transducer varies to some degree with frequency and the nominal linear range is a conservative value for any frequency at which the transducer is rated. The transducer

linearity may be improved by using the transducer at less than the nominal linear range. By using the MTS signal conditioning equipment, the transducers were calibrated at a nominal full scale range and at smaller ranges which provided increased linearity and resolution. The calibration of each range was checked at twenty points over that range. The maximum nonlinearity and hysteresis for the range was determined from these readings and the maximum for all ranges is shown in Table A2. This maximum difference generally occurred in the largest possible range, with increased linearity being shown at the finer ranges.

The smallest change that can be observed in the output of a transducer is called its resolution. Since the transducers used all operate on the principle of magnetic coupling, their theoretical resolution is essentially infinite and the limitation of the system resolution is in the ability of the associated electronic equipment to sense the output of the transducer. For the recording system used in these tests, the smallest value that could be conveniently monitored corresponded to a 1 mv output from the conditioner. The practical resolution for the system, as shown in Table A2 and listed on page 8 is based on the input measurement corresponding to a 1 mv output.

During the test series, the measurement system was periodically checked using known inputs and checking shunt cal voltages on the conditioners. The recorders were checked with known voltages before every test during the setup procedure, and system compliance was checked and accounted for before the test series began.

Table A1

Manufacturer Specifications for Transducers

Mode	Axial		Torsional		Both
Input Parameter	Load (lb)	Displacement (inch)	Torque (in-lb)	Angle (degree)	Pore Pressure (psi)
Nominal Linear Range	± 1000	± 0.1	± 500	± 60	0-250
Linearity and Hysteresis (% of full scale over total nominal linear range)	0.5% of full scale(*)	0.5% of full scale	0.5% of full scale(*)	0.1% of full scale	0.5% of full scale
Theoretical Resolution	infinite	infinite	infinite	infinite	infinite

(*) The linearity of the load and torque transducers are also rated at within 1% of the actual reading.

Table A2

Representative Specifications for Measuring System

Mode	Axial		Torsional		Both
Input Parameter	Load (lb)	Displacement (inch)	Torque (in-lb)	Angle (degree)	Pore Pressure (psi)
Peak Values for Range 1 ($\pm$ 10 Volts)	$\pm$ 1000	$\pm$ 0.1	$\pm$ 500	$\pm$ 50	0-200
Peak Values for Range 4 ($\pm$ 10 Volts)	$\pm$ 100	$\pm$ 0.01	$\pm$ 50	$\pm$ 5	0-20
Linearity and Hysteresis	$\leq$0.1% of total range being used	$\leq$.5% of total range being used	$\leq$.1% of total range being used	$\leq$.4% of total range being used	$\leq$.5% of total range being used
Practical Resolution for Range 4 (1 mv output)	1×10^{-2}	1×10^{-6}	5×10^{-3}	5×10^{-4}	2×10^{-3}

APPENDIX B

LIST OF SYMBOLS

The following symbols are used in this report:

a_t	threshold ground surface acceleration
B (B parameter)	pore pressure parameter
C_c	coefficient of curvature
C_u	coefficient of uniformity
D_r	relative density
D_{rf}	relative density after consolidation
D_{10}	diameter at which 10% of the soil is finer
D_{30}	diameter at which 30% of the soil is finer
D_{50}	diameter at which 50% of the soil is finer
D_{60}	diameter at which 60% of the soil is finer
E	cyclic (secant) Young's modulus
G_{max}	maximum shear modulus
J	polar moment of inertia
k_c	consolidation ratio = $\bar{\sigma}_{vo}/\bar{\sigma}_{ho}$
K_o	lateral stress ratio

NC	normally consolidated
n	number of cycles
OCR	overconsolidation ratio
p	$\frac{\sigma_1+\sigma_3}{2}$, $\frac{\sigma_v+\sigma_h}{2}$
$\bar{p}$	$\frac{\bar{\sigma}_1+\bar{\sigma}_3}{2}$, $\frac{\bar{\sigma}_v+\bar{\sigma}_h}{2}$
q	$\frac{\sigma_1-\sigma_3}{2}$, $\frac{\sigma_v-\sigma_h}{2}$
r	specimen radius
T	applied torque
u_r	residual pore pressure
ε_a	cyclic axial strain
ε_{at}	axial threshold strain
γ_c	cyclic shear strain
γ_t	threshold shear strain = 1.5 ε_{at}
$\bar{\sigma}_{ho}$	initial effective horizontal stress

$\bar{\sigma}_{vo}$	initial effective vertical stress
$\bar{\sigma}_{oct}$	initial effective octahedral stress $= 1/3(\bar{\sigma}_{vo} + 2\bar{\sigma}_{ho})$
$(\sigma_v)_{max}$	maximum axial load
$(\sigma_v)_{min}$	minimum axial load
τ_{max}	maximum shear stress